Thesis for The Degree of Licentiate of Engineering

Advancing quasar and satellite observations for VGOS

Rimsky Wolfs

Department of Physics and Astronomy
Chalmers University of Technology
Gothenburg, Sweden, 2026

Advancing quasar and satellite observations for VGOS

Rimsky Wolfs

Department of Physics and Astronomy
Division of Onsala Space Observatory
Space Geodesy and Geodynamics Unit
Chalmers University of Technology
SE-412 96 Göteborg,
Sweden
Phone: +46(0)31 772 1000

Cover:
Photo of the VGOS twin telescopes and the 25-meter telescope at the Onsala Space Observatory during a sunset in November 2025.

Printed by Chalmers Digitaltryck,
Gothenburg, Sweden 2026.

"All we have to decide is what to do with the time that is given us."
- Gandalf in The Lord of The Rings
by J. R. R. Tolkien.

Advancing quasar and satellite observations for VGOS

Rimsky Wolfs

Department of Physics and Astronomy
Chalmers University of Technology

Abstract

Very Long Baseline Interferometry (VLBI) is a space geodetic technique that contributes to the determination of the Earth Orientation Parameters (EOP) that are needed for the transformation between Earth fixed and space fixed reference frames. The VLBI Global Observing System (VGOS) is the newest development in geodetic VLBI with the aim of improving the determination of geodetic products to support the Global Geodetic Observing System's (GGOS) millimeter-level goals for reference frames to address Earth system challenges, such as climate change related sea level rise. However, so far the performance of VGOS is not yet at the millimeter-level due to mismodeling of error sources and (geo)physical phenomena.

One of the error sources that limits the ability to reach the VGOS performance goals is radio source structure; therefore, research is ongoing to better understand its impact and find ways to mitigate its effect. A proposed solution, as presented in this work based on real experiment data, is mitigating the source structure contribution by observing quasars only under certain favorable conditions, which can be guaranteed in 1-hour long VLBI intensive sessions that primarily determine the Earth rotation angle.

On a higher level, to obtain GGOS's millimeter-level goals, the determination of intra-technique biases between the 4 main space geodetic techniques is essential, since they impact the technique combination in the determination of the International Terrestrial Reference Frame. The Genesis mission of the European Space Agency aims at determining these intra-technique biases by launching a satellite that is observable by all 4 main space geodetic techniques. For this mission VGOS will be used to observe the Genesis satellite. Although some satellites have been observed with VGOS, many aspects remain to be tested and investigated. In this work, simulation studies of VGOS observations of Genesis are presented, related to precise orbit determination, satellite observation cadences, and simulation validations.

This research thus focuses on advancing both quasar and satellite observations for VGOS, by investigating real experiments that avoid source structure, and by assessing simulation studies in which satellites are being observed.

Keywords

Space geodesy, Very Long Baseline Interferometry (VLBI), VLBI Global Observing System (VGOS), quasars, source structure, satellites, Genesis

List of Works

Appended papers

This thesis is based on the following (under review) paper(s):

[**Paper I**] **R. Wolfs**, R. Haas, M. Schartner, M. H. Xu, and K. Le Bail, *Source Structure Informed Scheduling for VGOS Intensive Sessions*
Journal of Geodesy. Submitted, under review

Other works

The following work has been done during my PhD studies, but a manuscript has not been prepared. Therefore, they cannot be appended to this thesis, but are instead included in the thesis in a summarized form.

[**a**] **R. Wolfs** and R. Haas, *Simulating and analysing VGOS observations for Genesis orbits and EOP determination*
EGU General Assembly 2025, Vienna, Austria, 27 April - 2 May 2025, EGU25-19542, https://doi.org/10.5194/egusphere-egu25-19542.

[**b**] **R. Wolfs** and R. Haas, *A Hybrid Approach Using Real and Simulated Data to Assess the Performance of VGOS Sessions with Added Genesis Observations*
EGU General Assembly 2026, Vienna, Austria, 3–8 May 2026, EGU26-18316, https://doi.org/10.5194/egusphere-egu26-18316.

Acknowledgments

First of all, a special thanks goes out to my main supervisor Rüdiger Haas and co-supervisor Karine Le Bail. I am very happy that I have been given the opportunity to pursue a PhD with you as supervisors. You both have taken the time to meet with me, despite your busy schedules, to share your ideas, to provide insightful feedback, and to discuss the work and ideas with me. I am also grateful for the freedom that I have been given in terms of research, teaching, and faculty matters.

A heartfelt appreciation goes out to the current and former PhD students that I share and have shared an office with: Uttama, Rebekka, Yiting, and Alva. Talks about both work and life in the office and outside of it, and the together traveling to conferences, have made everything easier.

I want highlight the other fellow members of the space geodesy and geodynamics research unit, particularly Peng and Tobias, for their shared knowledge and feedback. Furthermore, the support from colleagues at the Onsala Space Observatory also needs to be mentioned and deserves recognition.

To all the fellow PhD students and non-PhD students in the GEO corridor, thank you for your company, whether it was during lunches or afterworks, the interesting and fun discussions were so welcome during and after work.

I also want to thank the geodetic VLBI community for the warm welcome, of which in particular my two co-authors Matthias and Ming Hui.

Finally, of course, I also want to thank my parents, sister, friends, and all the special people in my life for their love and understanding, of whom especially my mother because she must have heard about geodetic VLBI at least once per week.

Rimsky
Gothenburg, Sweden
May 2026

Contents

Part I

Summary

Chapter 1

Introduction

Why is a day 24 hours? How does a pizza delivery know where to go? How do we know that the sea level is rising? And, what do black holes have in common with these things?

These seemingly unrelated questions all have to do with the field of space geodesy that deals with measuring and understanding Earth's geometric shape, orientation in space, and its gravity field. With the use of geodetic techniques that involve satellites, telescopes, and specialized receivers, it is possible to do precise measurements that help in understanding the Earth system and answering questions about the cosmos.

The length of a day, related to the Earth's rotation, is deeply rooted in our daily life and the planet's ecosystem. Although a day is defined as being 24 hours, it is not constant and has shown a long term lengthening trend since the dinosaurs walked the Earth. As humans, we merely see a snapshot of the length of day through time, which is for us a fundamental given. The long term trend, and especially the short variations, in the length of day are known through the use of modern geodetic techniques, such as geodetic Very Long Baseline Interferometry (VLBI).

In case of the pizza delivery, the deliverer likely uses a specific navigation system to guide him/her to the destination. This navigation system is capable of providing the user with its location on the meter level, and with better equipment and methods, is able to do this even on the centimeter level. Systems that offer this capability are Global Navigation Satellite Systems (GNSS), which send signals that users can use to determine their location. GNSS is a space geodetic technique as well, which can also be used to measure the long term movement of stationary receivers that help to study the Earth's system.

The global sea level is rising due to the melting of large masses of, mostly polar, ice influenced by climate change. The global sea level is measured by special altimeter satellites that measure the distance from their orbit in space down to Earth. Only by knowing the location of the satellites precisely at centimeter level can conclusions be drawn on the measurements at centimeter level as well. The positions of the satellites can be determined very accurately at the centimeter level with the use of specialized space geodetic systems, such as GNSS, Doppler Orbitography and Radiopositioning Integrated by Satellite

(DORIS), and Satellite Laser Ranging (SLR).

Finally, black holes, being one of the largest and heaviest astronomical objects known to mankind, are the enablers of all the space geodetic techniques through their ability to serve as steady beacons in the furthest reaches of space. Through them, when in their most active form known as quasars, geodetic VLBI is able to determine the absolute orientation and rotation of Earth in space, which is needed to make all geodetic satellite systems work accurately.

* * *

This thesis focuses on the geodetic technique VLBI. In particular, the most recent developed VLBI Global Observing System (VGOS), which aims at supporting the millimeter level requirements set by the Global Geodetic Observing System (GGOS). That requirement was set to address future Earth system challenges and natural hazards impacts by being able to make informed Earth observation based decisions. Although the performance of VGOS is better than its predecessor, it is not yet at the millimeter level due to mismodeling of error sources and (geo)physical phenomena.

In this thesis two topics are investigated, advancing quasar observations and satellite observations in VGOS. The first topic is on mitigating radio source structure effects in VGOS intensive sessions. Radio source structure is shown to introduce errors at the few millimeter to centimeter level. An analysis is presented using two VGOS intensive session series of which one was scheduled with a constraint that should mitigate the effect of radio source structure by only observing quasars in certain favorable conditions. The second topic is satellite observations with VGOS, for which both real and simulated data have been used. With the upcoming Genesis mission from the European Space Agency (ESA), which will be observable by all 4 space geodetic techniques, there is a lot of insight needed from the VGOS point of view. Two brief overviews of analyses are presented in which Genesis observations by VGOS are simulated and analyzed, and the impact on estimated station positions, Earth orientation parameters, and the satellite orbit are investigated. This gives insight on the expected precise orbit determination performance and the impact of incorporating satellite observations in VGOS sessions on geodetic parameter estimation.

The thesis outline is as follows: Chapter 2 provides an introduction to space geodesy, the scientific field to which VLBI and VGOS belong, shedding light on different space geodetic techniques, reference systems, and reference frames. Chapter 3 gives an in-depth overview of geodetic VLBI by laying out the basic principles, explaining the systems used and session types observed, explaining the whole measurement chain from scheduling to analysis, and ends with an overview of simulations and their validations. Chapter 4 lays out the groundwork more specifically on the two main topics that the research in the thesis is dealing with, namely quasars with their radio source structure which affects VGOS observations, and satellite observations within VGOS, which are for the upcoming Genesis mission a main topic of further investigation. Chapter 5 is the final chapter of the thesis and gives the summaries of the appended paper and research work done, and provides a hint at what work is to be done in the future.

Chapter 2

Space geodesy

Author note: This chapter gives an overview of space geodesy. Before I will talk about geodetic VLBI it is important to know what the space geodetic field contributes to society and the world, how VLBI fits in with the other geodetic techniques, and what geodetic products are generated by the geodetic community.

Geodesy is the scientific field that deals with the measurement of the gravity field, shape, orientation, and rotation of Earth. The gravity field of the Earth is constantly changing due to moving water, ice, and land, as well as the interior of the Earth. Also the rotation of the Earth has an influence on the gravity field of the Earth; more mass is located at the equators than at the poles. This means that based on gravity measurements we can conclude something about the mass movement on and inside the Earth. The shape of the Earth is influenced, mainly, by surface erosion due to weather and water, and by geodynamic processes. Finally, Earth's orientation and rotation change all the time, mostly in a consistent periodic way, but biases and small deviations exist, especially for the Earth rotation.

Although geodesy is not readily known by everyone, every part of society uses geodetic systems in some way or another, by allowing global positioning and time synchronization (Angermann et al., 2022). Geodetic satellite systems enable navigation and logistics based services such as smartphone navigation, deliveries, aviation, autonomous driving, and precision agriculture, and provide precise time distribution used by financial and telecommunication services, such as banks, mobile networks, and the internet. On a higher level, scientific and environmental fields, such as astronomy, disaster management, and climate change monitoring (through, for example, sea level rise) are all making use of geodetic measurements and products. It is therefore safe to say geodesy is located at a societal and scientific fundamental level, at least nowadays.

Geodetic measurements of the Earth date back as far as the Romans and Egyptians (Angermann et al., 2022). For example, the circumference of the Earth was already estimated correctly to a few hundred kilometers off by Eratosthenes in ancient Greece. Over the last few millennia geodesy has evolved from very local measurements to more profound and encompassing methods that allow for the accurate measuring of vast areas with high precision. Methods

and instruments such as triangulation, gravimeters, sextants, compasses, and more have been established. However, since the 1960s a new form of geodesy has been making its way into the field, which makes extensive use of methods that use space, which we call space geodesy.

Space geodesy is a subfield of geodesy that conducts geodesy using space based techniques. Space geodetic techniques (Section 2.1) allows geodesy on a planetary scale, by using satellites, the Moon, and radio wave emitting extragalactic sources called quasars (quasi stellar radio sources). Some geophysical processes and dynamics have only been proved by the use of space geodetic techniques, such as for example plate tectonics. Space geodesy is used to determine, among others, reference frames (Section 2.2), such as the International Terrestrial Reference Frame (ITRF) (Altamimi et al., 2023), which is an Earth fixed reference frame based on geodetic station positions and velocities, and the International Celestial Reference Frame (ICRF) (Charlot et al., 2020), which is a space fixed reference frame. Also, the connection between the two is determined in the form of the five Earth Orientation Parameters (EOP, Section 2.2.2).

2.1 Space geodetic techniques

Within the field of space geodesy, four major techniques are considered:

- Very Long Baseline Interferometry (VLBI)
- Global Navigation Satellite Systems (GNSS)
- Doppler Orbitography and Radiopositioning Integrated by Satellite (DORIS)
- Satellite Laser Ranging (SLR)

It is important to note that all of these techniques use electromagnetic waves to make their observations. In three of the cases a time delay is being measured and in one case a frequency change is measured of the electromagnetic waves' frequency. At the core of all of them is the speed of light, which is currently defined to be 299,792,458 meters per second and dictates the speed at which electromagnetic waves move in vacuum.

VLBI uses quasars to determine the positions of telescopes relative to each other, EOPs, and quasar positions for the ICRF, using experiments that can last 1 to 24 hours, or even several days. Since more on VLBI is given in Chapter 3, we limit the further in depth discussion of VLBI here. The International VLBI Service for Geodesy and Astrometry (IVS) (Nothnagel et al., 2017) is the main body that conducts geodetic VLBI experiments.

GNSS consist of constellations of satellites primarily in medium Earth orbit that emit accurate time tagged radio signals. Usually two different radio frequency signals are used, called L1 and L2, which are needed to correct for ionosphere induced delays of the signals. The time signals are time tagged by using atomic clocks on board of the satellites. The radio signals can be picked up by receivers on Earth or in space, which can use trilateration to determine

their position by calculating the distances to each of the satellites based on each satellite's respective signal, which includes the satellite's position and time of transmitting the signal. At least four signals need to be received at the same time to get an estimation of the position and time. The time also needs to be solved for since receiver clocks are usually not stable, therefore, they need to be synchronized with the satellite constellation time to get a meaningful result for the position determination. Many billions of GNSS receivers are present on Earth's surface, such as in phones, but for geodesy usually high grade GNSS receivers are used. Also many satellites have GNSS receivers on board, which are used to determine their orbits (see also Section 4.2.2). The advantage of using GNSS is that there are many continuous signals available that can be used to determine to orbit of a satellite. Notable GNSS constellations are Galileo, GPS, GLONASS, and BeiDou, as well as regional constellations such as QZSS and IRNSS. The International GNSS Service (IGS) (Johnston et al., 2017) is the main body that organizes the GNSS efforts for geodesy.

DORIS uses a network of well distributed ground stations (beacons) that emit radio signals on two different radio frequencies, again, like for GNSS, primarily to correct for the signal propagation error due to the ionosphere. These radio signals are picked up by satellites that have a DORIS receiver on board which includes an atomic clock. Instead of measuring delays, DORIS measures the Doppler shift of the received signals, with the primary goal of determining the orbit of the satellite. In order to determine the Doppler shift accurately and avoid Doppler collisions, preferably only one station should be visible at a time, though the newest version of the DORIS receiver can support up to 7 beacons (the amount a satellite observes at about 1330 km altitude) at any one time (Auriol and Tourain, 2010). Furthermore, the signals emitted need to be very stable and the receiver needs to have a very accurate frequency standard. Using the Doppler measurements over multiple orbits, the satellite orbit can be solved for, as well as the station positions and velocities. Many remote sensing satellites in low Earth orbit (LEO) have a DORIS system on board to estimate precise orbits, which are generally needed in order to get accurate satellite or payload measurements. The International DORIS Service (IDS) (Willis et al., 2016) is the main body that organizes the DORIS efforts for geodesy.

SLR uses accurately timed laser pulses sent from ground stations to retro reflectors on satellites (or on the Moon) and determine the distance to the object based on the time it takes for the reflected signal to come back to the ground station. This is thus a two-way measurement and only needs an accurate clock on the ground. Another advantage is that on board the satellite no active components are needed. Examples of SLR satellites are LAGEOS and LARES, which are passive satellites consisting of a spherical shape with only retro reflectors on their surface, at about 6000 km and 1400 km respectively. These satellites are primarily used to determine the spherical harmonics of the Earth's gravity field as well as to conduct some specific scientific experiments. Many remote sensing and GNSS satellites also have SLR retro reflectors on board, which can be used to validate the determined orbits from the other techniques. The International Laser Ranging Service (ILRS) (Pearlman et al.,

2019) is the main body that organizes the SLR efforts for geodesy.

Three important associations and services should be mentioned where the four main space geodetic techniques contribute to. Firstly, the International Association of Geodesy (IAG), whose mission is to advance geodesy through research, data analysis, technological development, and providing accurate representations of Earth and planetary systems (IAG Office, 2025). Secondly, the Global Geodetic Observing System (GGOS) (Plag et al., 2010), which was established in 2023 as part of the IAG, is the metrological basis for global change research and investigates global deformation and mass exchange within the System Earth consisting of solid Earth, hydrosphere, atmosphere, and cryosphere. Third and finally, the International Earth Rotation and Reference Systems Service (IERS)[1] which primary objective is to serve the astronomical, geodetic and geophysical communities by providing data and standards related to Earth rotation and reference frames.

Finally, there are some geodetic satellites that are worth mentioning, which all did gravity measurements of the Earth. GRACE (Gravity Recovery and Climate Experiment) is a series of satellites pairs that orbit 200 km behind one another and very precisely keep track of the distance between them. Their measurements are sensitive to Earth's gravity field; the first satellite is impacted first, and the second satellite after. This way a differential measurement of the gravity field can be made. CHAMP (Challenging Minisatellite Payload) was a satellite mission that primarily measured Earth's ionosphere, but also did measurements on Earth's gravity field and radio occultation. GOCE (Gravity Field and Steady-State Ocean Circulation Explorer) was a very low altitude orbiting satellite, at about 255 km. The primary objective was to make high spatial resolution and sensitive measurements of Earth's gravity field and Earth's geoid.

2.1.1 Local and space ties

An important aspect is that each geodetic technique can produce its own solution for a reference frame (more on this in Section 2.2). Each technique also differs and produces slightly different results. In order to find intra technique biases (or systematic differences) local ties can be used. Local ties are geometrical measurements of different techniques that operate in the same local environment. An example of a local tie is a GNSS receiver and a VLBI telescope standing next to each other. Since they are close together one can assume that they experience the same local geophysical phenomena, the same atmospheric effects, and the same physical environment. Such a local tie allows, if known precisely, the tying of the two techniques together on global scales, where the local ties act as connection points.

Only a total of five local ties exist in the world that have a good record of all four space geodetic techniques, namely Washington (USA), Hartebeesthoek (South Africa), Yarragadee (Australia), Metsähovi (Finland), and Wettzell (Germany). About 12 local ties exist between three techniques, and about 55 unique local ties sites exist between any two techniques (Seitz et al., 2026). This

[1] International Earth Rotation and Reference Systems Service, https://www.iers.org/

is mostly limited by non-GNSS techniques, since almost all geodetic observation sites have a GNSS station.

In order to achieve the goal of GGOS to produce reference frames that are accurate to the 1 mm level and stable at 0.1 mm/year, it is considered essential to determine the biases between the four space geodetic techniques more precisely (Delva et al., 2023). This is not possible using only a handful of local ties, which, due to some limitations of the space geodetic techniques, cannot easily be increased in number. Therefore, ideas exists to launch a satellite that can be used by all four space geodetic techniques to supply space ties instead (Bar-Sever et al., 2009; Biancale et al., 2017; Rizos and Willis, 2014). If a satellite orbit is chosen that is not geostationary, in theory almost all space geodetic stations in the world at some point can observe it and be "linked" to this one satellite, thereby creating one space tie between all four space geodetic techniques through time. Such a satellite mission has been accepted by the European Space Agency (ESA) and is called Genesis (Delva et al., 2023) (for more on Genesis see Section 4.2.4). The Genesis satellite, as of writing, is to be launched in 2028 and will be observable by all four space geodetic techniques, allowing for the creation of the aforementioned space ties between the techniques.

2.2 Reference systems and reference frames

To indicate where things are seems simple, but to get an accurate way of describing this with numbers is more difficult. Furthermore, how can we ensure that different mentions of locations produced by different entities end up at the same place? For this, we use reference systems and reference frames.

A reference system is a definition of how a set of (usually) orthogonal axes should be defined in space and time. Different reference systems exist that have their origin in different places, such as the center of the Earth, the solar system barycenter, the Sun itself, other planets, and so forth. Next to the origin, also two out of the (usual) three axes need to be defined. The z-axis is usually is set to be aligned with a rotation axis, for example the rotation axis of the Earth, or the momentum vector of the solar system (which points "up" from the ecliptic). Then the x-axis is usually taken as the pointing towards a fixed point in space, or is fixed to the rotating body it is defined for. The y-axis usually completes the right hand system. A realization of such a system, meaning a physically accessible set of points and their coordinates in that system, is called a reference frame.

Both fixed and inertial reference systems can be defined. For example, in geodesy we deal with the Earth, so we can have an Earth Centered Earth Fixed (ECEF) system, thus a system that rotates with the Earth, and Earth Centered Inertial (ECI) system, a system that does not rotate with Earth. The last named frames are not scientific frame names, but are used frequently to give an indication of what kind of system one talks about.

In terms of scientifically namings of reference frames, we have so called celestial and terrestrial reference frames. Celestial systems and frames are fixed

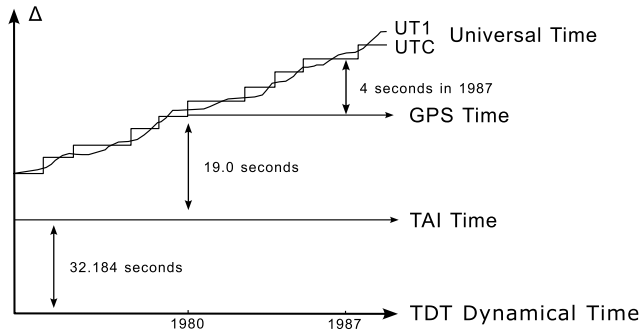

Figure 2.1. Different time scale comparisons, remake from (Seeber, 1993).

w.r.t. the astronomical objects, i.e. their x-axis points to a specific point in space, and terrestrial systems and frames are fixed w.r.t. the Earth, i.e. their x-axis points through a physical point on Earth, such as the prime meridian. For Earth, following the rules of the International Terrestrial Reference System (ITRS) an ITRF can be realized. Depending on the data used (for example only GNSS or only VLBI data, or a full combination of all four space geodetic techniques), different versions of such a reference frame can be made. For example, the ITRF version of 2020 uses data from four major space geodetic techniques, while the VTRF (VLBI Terrestrial Reference Frame) uses only data from VLBI measurements. The different ITRF realizations can be found at the Institut National de l'Information Géographique et Forestière (IGN) ITRF webpage [2].

To transform between reference frames one needs transformation parameters that are usually a function of time, such as the earlier mentioned EOPs.

2.2.1 Time and timing

Time keeping seems a trivial thing. However, when dealing with delay measurements of electromagnetic waves, whether it is light or infrared in SLR or radio plane waves in VLBI, a small difference in timing can lead to vastly different calculated distances due to the large magnitude of the speed of light. For example, a measurement error of 10 nanoseconds (10×10^{-9} s) leads to a distance error of about 3 meters. Therefore, using the same time scale and an accurate way to keep it consistent between multiple locations are detrimental for the ability to conduct space geodesy.

Different time scales exist, such as Universal coordinated time (UTC), universal time (UT1), and international atomic time (TAI) (see Figure 2.1).

UT1 is purely based on the rotation of the Earth, defined as when the Sun crosses the prime meridian at 0° longitude. UTC aims to follow UT1, however its timescale is defined by atomic clocks like TAI, and has thus to be kept to within 1 second of UT1 using leap seconds, so that UTC continues to correspond to time determined by Earth's rotation. Since 1970 about 27 leap

[2]IGN ITRF webpage, https://itrf.ign.fr/en/homepage

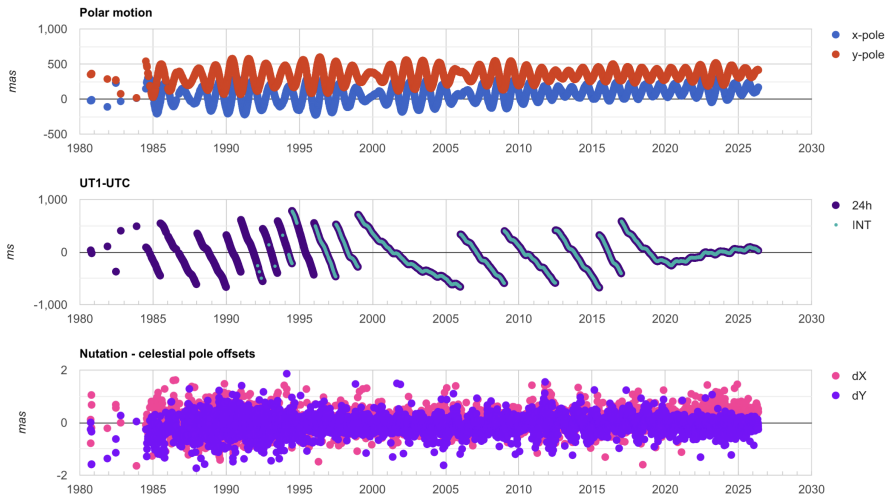

Figure 2.2. Timeseries of the five EOP as determined by the Vienna Center for VLBI.

seconds were introduced to keep UTC aligned with UT1. The addition of leap seconds is primarily due to the slowing down of the rotation of the Earth. This is caused primarily by tidal friction with the Moon, but is also influenced by, for example, the mass redistribution of melted ice and the climate anomaly El Niño (Angermann et al., 2022).

Time keeping becomes especially complicated under relativistic effects which causes clocks to run at different speeds. This means for example that GNSS satellites, at altitudes of around 20,000 km, need to adjust their clock rates to make sure that they run at the same speed as Earth based clocks (Ashby, 2003).

2.2.2 Earth Orientation Parameters

A complete transformation between two different reference frames in 3D can in general be achieved with seven transformation parameters. In some cases in geodesy the Helmert transformation is used which consists of three translations, three rotations, and one scale factor. A more common use case which is important for (space) geodesy, is the transformation between ITRFs and ICRFs, which is governed by the five Earth orientation parameters. Using this method there are however no scale and translation transformations applied.

The five EOPs are the X and Y components of the celestial pole offset, the Earth rotation angle, and the X and Y components of polar motion, and are linked to physical phenomena that the Earth exhibits, being nutation, precession, rotation, and polar motion. See Figure 2.2 for the five EOP timeseries as determined by the Vienna Center for VLBI[3]. The celestial pole

[3]VLBI https://www.vlbi.at/products/

offset describes how the Earth rotation axis changes w.r.t the ICRF, thus "the stars". The Earth rotation angle is described as the difference between UT1 and UTC, an offset between the two time scales. If UT1 is related to the ICRF, when the Sun passes the prime meridian, and the UTC day is defined as 86400 seconds and related to atomic clocks, the difference UT1-UTC tells how much the Earth rotation is different from the when those two would be exactly aligned. One can convert the difference UT1-UTC in time to an angle, the Earth Rotation Angle (ERA), by using the fact that the Earth rotates 360° in 86400 seconds, which is 15 arcseconds per second, in UTC time. The polar motion describes how the Earth's crust moves w.r.t. the rotation axis. The three parameters of Earth rotation and polar motion together are known as Earth Rotation Parameters (ERP).

Another parameter related to the EOPs, called the length-of-day (LOD), is sometimes also used. It describes how long it takes the Earth to do one rotation around its axis and thus only indicates something about the change in UT1-UTC (its rate), but not about the UT1-UTC absolute value. This parameter is usually determined by geodetic satellite systems (so all except VLBI), which are sensitive to Earth's rotation but are not tied to the ICRF.

All EOPs can be determined by VLBI, whilst all except the UT1-UTC parameter can be determined by the other three space geodetic techniques. Furthermore, GNSS needs the UT1-UTC value to function properly. Therefore, VLBI is essential to determine all five EOPs.

Chapter 3

Geodetic Very Long Baseline Interferometry

Author note: This chapter gives an overview of how geodetic VLBI works. It is important to show the basics of this system since it is the primary system used in the presented research. Since the presented work is heavily leaning towards the analysis part of the geodetic observations, the emphasis in this chapter is on that part of the whole geodetic parameter production chain.

Geodetic VLBI is a complex method and in this chapter only a general overview is given of the technique. The interested readers are further pointed towards the works by Sovers et al. (1998), albeit a bit dated still relevant and very comprehensive, and Schuh and Behrend (2012).

If one looks in literature and elsewhere, one will find that VLBI is used in two main scientific fields: astronomy and geodesy (Moran, 1998) . VLBI was first used primarily for astronomy, for which it was envisioned to allow for extreme high resolution images in the radio regime by taking advantage of telescopes at distances larger than one single telescope could be built. At first this meant telescopes several hundreds of meters apart, but later this method would also be applied to telescopes being as far apart as the Earth's diameter would allow. This because the resolution of a radio telescope is determined by the ratio of the wavelength over the diameter D, or baseline length b, of the telescope or interferometer.

$$\theta \equiv \frac{\lambda}{D} \equiv \frac{\lambda}{b} \tag{3.1}$$

This allowed for the imaging of a single source of interest with unprecedented detail, using arrays of multiple telescopes separated by several to thousands of kilometers.

However, if one would not be interested primarily in observing the astronomical source, but would instead observe an almost point like source, one can use an interferometer for a different cause. Instead of focusing on the astronomical data in terms of so called visibilities, one can instead focus on the time delay

between the telescopes of the signal arriving from the source. Together with the speed of light we can obtain a geometric distance measurement between the involved telescopes. This method is used in geodetic VLBI to determine telescope locations and EOPs, and was for the first time conducted for that purpose on a transatlantic baseline between a telescope at the MIT Haystack Observatory in Westford, Massachusetts, USA, and one telescope at the Onsala Space Observatory in Sweden in the late 1960s (Moran, 1998; Ryan et al., 1986; Whitney, 1974).

A subfield of astronomy that uses the same measurements as geodetic VLBI is astrometry, which focuses primarily on locating the observed astronomical sources in the ICRS.

3.1 The principle of geodetic VLBI

In Section 2.1 VLBI was only briefly described to use quasars to determine station positions, EOPs, and optional quasar positions. At its core VLBI uses natural noise to determine differences in arrival times between telescopes, and is therefore different from GNSS, SLR and DORIS in the sense that is the only technique that uses natural radio sources. Furthermore, VLBI is the only technique that can tie the ICRS and the ITRS together in an absolute sense, as it is the only technique that can measure "the stars" relative to the Earth, and is the only technique that can measure the Earth rotation angle (ERA) w.r.t. the ICRS.

To understand how VLBI works, lets first start with what the method actually measures. Consider two telescopes on the surface of the Earth, at a reasonably large distance apart at, for example, a 1000 km. These two telescopes form a baseline $\vec{b}$, see Figure 3.1. Both of these telescopes are set to look at an extremely far away radio source, called a quasar (see more on quasars in Section 4.1), in the direction of $\vec{k}$. For now, one may assume that a quasar is an astronomical object far away outside of our own Milky Way galaxy, and therefore appearing very point-like. The quasar emits strongly in the radio part of the electromagnetic spectrum and this emission is random noise. Due to quasars being so far away, multiple fair assumptions can be made about quasars when observed from Earth: they are point-like, they are stationary against the celestial sphere, and their emitted radiation arrives at Earth as a plane wave. When the

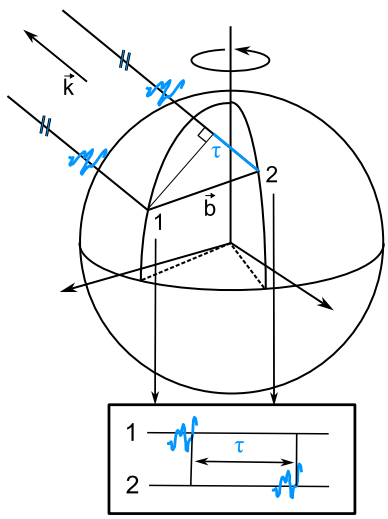

Figure 3.1. The principle of VLBI. Inspired by similar figure from J. Böhm.

plane wave arrives at Earth, it will first reach the closest telescope to the quasar and after that the second telescope. The plane wave signal is time tagged at each of the telescopes when it arrives, using an atomic clock, and recorded on special recording computers. It should be noted that, given that the quasar signals are typically very weak when they reach Earth, the signals need to be recorded for typically 20 - 120 s in order to achieve a reasonable signal-to-noise ratio (SNR). Now, after the recording has finished, the recordings of each of the telescopes can be cross correlated with one another by a special computing facility called a correlator. In this method the recordings are shifted in time to find how much time there is between the arrival of the noise plane wave at telescope 1 and telescope 2. The found time difference is called the delay and is thus a measure of the time, or approximate distance using the speed of light, between the telescopes projected towards the observed quasar. This time delay is the elemental observable of geodetic VLBI.

Having only one single delay on its own is not very useful. However, such a time delay measurement can be repeated for several different quasars, given that the quasars are visible to both telescopes. For example, 10 different quasars can each be observed in 10 minutes by two telescopes, leading to 10 measured time delays. This thus leads to a collection of precise time delays between the two telescopes projected towards different geometrical directions as dictated by the observed quasars. Again, no actual distance is measured to the quasar, but only a time difference between the two telescopes in the direction of the quasar. This collection of measurements holds information on how these two telescopes move w.r.t. the observed quasars.

To understand this better, lets use an example of the Earth with the two telescopes on it, e.g. one in Sweden and one in Japan. Around it is an outer sphere with the quasars, which stands completely still forming an inertial reference system, the celestial sphere. The Earth is tilted and rotates around its rotation axis. First, the telescopes observe a quasar in a certain direction on the celestial sphere for about 60 seconds and the first time delay can be determined. Then, a second quasar in another direction on the celestial sphere is observed for 60 seconds, leading to a second time delay. In the mean time the Earth has rotated, so the two telescopes have slightly moved w.r.t the outer celestial sphere with quasars. We can repeat this process for a large amount of quasars. For example, we can do this for 24 hours, which means the telescopes are again, after one day, back at the point where they started w.r.t. the outer sphere with quasars. Now, if we assume that the outer sphere with quasars does not move, the quasars themselves have known locations, the telescopes do not move on the Earth surface, and the only movement is the Earth rotation, we can find the actual rotation speed of the Earth by fitting a rotation model to the time delay measurements.

The 2 telescope setup that has been explained in the example above is close to a so called VLBI "intensive session" or experiment. The only difference is that in the actual intensive sessions the duration is just one hour. What is the same is that such an experiment is conducted primarily to determine the rotation of the Earth.

Now, of course it would be ideal to determine all five EOPs and not just one.

This is possible if we increase the number of telescopes in the experiment from two to multiple telescopes (called a network) that are spread out all over the Earth. In that case the amount of time delays that are measured between each pair of telescopes increases quadratically and not only the Earth rotation can be estimated, but also the celestial pole offsets (the orientation of the Earth in space) and the polar motions (the movement of Earths crust relative to the rotation axis) can be determined. Furthermore, if the network is large enough also the telescope positions and a selected amount of quasar positions can be estimated. Such experiments are usually conducted over a period of 24 hours.

3.2 System and session types

Within the IVS different two different VLBI systems are used and many different session (or experiment) types exist, which both will be discussed in the next two sections.

3.2.1 Systems

Before we dive into the observing, processing, and analysis of the VLBI measurements it is important to make a distinction between two types of geodetic VLBI observing systems: the older so called legacy S/X system and the newer VLBI Global Observing System (VGOS).

The legacy S/X system consists of different types of telescopes, which were almost all originally designed for astronomy purposes (Moran, 1998). This means that all these telescopes are all very different in terms of size, slewing (rotation) speeds, recording systems, operational bandwidths, structural integrity, and so forth. All these differences are in their own way disadvantageous in observing quasars for geodetic purposes. For example, different slewing speeds means that some telescopes take long times to slew from quasar to quasar while the other telescope is already ready for observing a quasar, and different structural integrity means that some bigger telescopes deform more than others under their own weight, which needs to be accounted for later on in the analysis since it alters the measured time delay. Another important aspect is that this system only records in two bands: S and X band. In this system two frequency bands are needed to correct for ionosphere induced time delays.

The VGOS system aims to be a homogeneous network of telescopes, primarily designed for geodetic VLBI observations (Petrachenko et al., 2012a), and is part of GGOS. See Figures 3.2 and 3.3 for an overview of the current VGOS network (some telescopes are not shown to avoid clutter, indicated with a number in brackets behind the name) and some soon to be included stations. The telescopes are mostly 12 - 13 meters in diameter, can all slew at relative high speeds, all have similar recording backends, are all capable of observing in four different frequency bands, and are equipped with broadband receiving systems (Schuh and Behrend, 2012). All these improvements w.r.t. the legacy S/X system allow for better troposphere estimation, direct elimination of the ionospheric delay, a finer delay resolution, and more effective bandwidth syn-

Figure 3.2. Current (red) and future (white) VGOS stations as seen from over Asia.

Figure 3.3. Current (red) and future (white) VGOS stations as seen from over the Americas.

thesis (Sovers et al., 1998). Furthermore, the measurement noise is expected to be a magnitude lower than in the legacy system.

Despite some initialization issues in VGOS and some new challenges that have been brought to light (Xu et al., 2022; Zubko et al., 2025), the system has proven to outperform the legacy system in terms of precision and EOP products (Haas et al., 2021; Nilsson, 2022; Wang et al., 2022).

A new identified challenge for VGOS is the increased sensitivity to radio source structure of quasars (Section 4.1) due to the higher and more frequencies observed and the system having less measurement noise (Xu and Charlot, 2025; Xu et al., 2021a; Xu et al., 2022), Furthermore, the ambiguity spacing has been reduced to only $\sim$ 316 ps, which is hypothesized to cause problems in the fringe fitting process due to the ionosphere introduced delays being on the same order of magnitude (Zubko et al., 2025).

For the rest of this work the focus will be primarily on the VGOS system.

3.2.2 Sessions

Within the IVS different types of experiments (or called sessions or series) are observed. Most of these experiments are focused on geodetic and astrometric measurements.

In general for the geodetic experiments there are two types in terms of experiment lengths: standard 24 hour sessions and 1 hour intensive sessions.

Main operational 24 hour sessions that are primarily used to determine the EOPs, are global sessions that use a large networks of typically 6 - 15 telescopes. The legacy S/X operational sessions are called R1 and R4 and are each observed about once every week on different days (McCarthy and McCallum, 2025). For VGOS the operational sessions are called VGOS-OPS and are observed once every week in 3 weeks per month, and every week since 2026. The lower cadence of the VGOS-OPS sessions has to do with the large data volume generated per experiment. This leads to a latency of more

than 30 days on average for the VGOS-OPS sessions between observing and publishing the derived EOPs. This consequently means that the VGOS-OPS data is currently not used in the IERS rapid products, but only in the final ones. Other 24 hour sessions exist with, for example, the focus on research and development, or the determination of the ITRF or ICRF.

The 1 hour intensive sessions, which are observed by 2-3 telescopes on east-west baselines, are a compromise; they do not generate a lot of data and thus have typically a low turnaround time, but due to only using a few telescopes can only supply the Earth rotation parameter UT1-UTC. These intensive sessions are primarily important for GNSS, satellite operations, and other fields in which a regular updated accurate value of the most variable EOP, the Earth rotation angle, is of importance. Several different intensive session series exist divided between the legacy S/X and VGOS systems.

Other sessions exist that do not fit within the boundaries mentioned above. Many of those sessions are experimental and do not have a high amount of reoccurrence.

3.3 Observing and processing measurements

Before going into depth on how the actual EOPs and station positions can be estimated in the analysis step, it is good to know how the observed time delays are found based on the observations of the noise coming from quasars. In the next sections overviews of scheduling, observing, correlation, and fringe fitting are given.

Scheduling

Before observing a geodetic VLBI experiment, an observation plan, called a schedule, has to be prepared. This is usually done using *Sked* (Gipson, 2010, December) or *VieSched++* (Schartner and Böhm, 2019), which both allow the automatic generation of observation schedules given inputs and criteria.

In both scheduling programs, the general idea is the same: find an optimal way to observe quasars to determine the parameters of interest (EOP, station positions, and/or quasar positions). The scheduling process takes into account at least the date, time, and duration of the experiment, the telescopes involved, the slew rates of the telescopes, the frequency setups used, and the quasars that are allowed to be observed. Here also the session or experiment type plays a role; 1 hour 2-3 station intensive sessions have slightly different requirements than 24 hour 6+ station global experiments. In addition to the basic settings, many additional optimization criteria can be added, especially in *VieSched++*. A handful of examples of such optimizations are: Allow subnetting of a certain amount of telescopes (meaning that subgroups of the total telescope network are allowed to observe different quasars), give weights to certain baselines, quasars or telescopes, add a number of calibration scans (these scans can be used to help the fringe fitting process), include a certain amount of observations in certain parts of the sky, and/or using signal-to-noise ratio (SNR) based

scheduling (which limits the observing time for each quasar such that just a sufficient SNR is reached).

Once a schedule is made it is distributed by SKD (Gipson, 2010, December) or VEX (Vlbi EXperiment) (Whitney et al., 2002) files either directly to the involved telescope observatories or via an organization such as the IVS.

Observing

Before the observations can be made by the telescopes in an experiment, the telescope and its systems need to be set up to do the work automatically. For this, the schedule has to be downloaded, which with the use of a series of scripts from the field system (FS) (Himwich, 2000) can be converted to get the telescope's specific planned observations and accompanying settings that the telescope system can use to steer the telescope during the experiment. Once the experiment has started, each planned observation for the telescope is made in timely manners, which due to the schedule is synced with one or more telescopes elsewhere in the world observing the same quasar.

In each quasar observation the electromagnetic waves are reflected by the antenna, which for VGOS contains typically one main and one sub reflector, and focused into the feedhorn after which it is converted into an electric voltage signal (RF) and amplified by a (typically) cryo-cooled Low Noise Amplifier (LNA). At this point also an artificial phase calibration (phase-cal) signal/tone is injected into the signal, which allows for phase calibration later in the fringe fitting process (see Section 3.3) which is part of the overall observation processing chain. After further amplification the RF signal is down converted to an intermediate frequency (IF) and enters, in some cases as for the OTT over a 1 km long optical fibre cable, a digital back-end (DBE, such as a digital baseband converter like DBBC3) where the signal is split up into channels per frequency band. In case of VGOS this means 8 channels of each 32 MHz at frequency bands A, B, C, and D, in two polarizations. Here the frequency bands are roughly at, depending on the actual settings, 3, 5, 8, and 10 GHz. Then each IF signal is converted to baseband frequencies and digitized at the chosen quantization level. Here also a time tag is added based on the pulse-per-second signal from a stable atomic clock at the respective observatory, typically a hydrogen maser, and formatted and transferred to a recorder (such as a FlexBuff) which is usually on site, but could also be directly transferred to a remote location.

Correlation

After the experiment the data of all the telescopes in one experiment is transferred to an institute, high computing facility or similar, called a correlator. Currently, especially for VGOS, this transfer step is one of the main bottlenecks in terms of turnaround time of each experiment, since in the case of VGOS a 24 hour experiment generates about 25 TB of data per telescope. Depending on the internet speed it can thus take up to a few days or a week to transfer the data from all the telescopes to one correlator.

Once all the data is present at the correlator the actual cross-correlation of the data can start. Two different approaches can be used in the correlation step; either (1) first the cross-correlation is done after which the Fourier transform is taken, or (2) first the Fourier transform is taken after which the cross-correlation is done. Both approaches have their advantages (Nothnagel, 2019), but nowadays mostly the Distributed FX (DiFX) correlator software is used, which first takes the Fourier (F) transforms using the Fast Fourier Transform (FFT) algorithm, after which cross-correlation (X) is done (hence the FX in the name).

To understand the process that is happening in the correlator, it is easier to look at the XF method. In that case, first for each baseline, each observation is cross-correlated between the two telescopes to find the time delay τ between the signal arrival times from the observed quasar. This is done by shifting the signal in time of one of the two telescopes relative to the other telescope until the cross-correlation function is maximized (Sovers et al., 1998). After this the FFT is applied to the cross-multiplied shifted signals and the complex visibilities for each band, polarization and baseline are obtained. In the FX method these two steps are switched, but lead to the same results.

After the cross-correlation and FFT steps have been performed the complex visibilities are time averaged for each chosen time step interval and are saved. We have obtained the complex visibilities per observation, baseline, band, and polarization. However, we would like to have one so called group delay per observation and baseline, thus we need to make a consistent grouping of the data, which is achieved during fringe fitting.

Fringe fitting

Fringe fitting is the final step in the processing of the raw VLBI observations, complex visibilities, and aims to obtain the group delay per observation and baseline. For this, usually the *fourit* software from the Haystack Observatory Pos-Processing Software (HOPS) is used. The bandwidth synthesis technique comes into play in this step (Sovers et al., 1998) and the previous injected phase-cal signal data is now used to correct the phases in each single channel.

The inputs for fringe fitting are the corrected complex visibilities per observation on a baseline, band, and polarization. A two dimensional FFT of the cross-correlation spectra is used to find the peaks of the function in frequency (group delay) and time (delay rate) domains. The peaks found in the delay and delay-rate domains supply the a priori values for the bilinear least-squares, which determines the observables ϕ_0, τ_{gd}, and τ_{pd} (phase, group delay, and phase-delay rate).

Once the group delays are determined they can be written to a database like vgosDB (or NGS in the past). In addition, other information and data are written in the database as well, such as local meteorological measurements, cable calibration, and event logs of the telescopes. The database is then distributed to be used for the actual analysis, in which the parameters of interest, such as EOPs, can be estimated.

3.4 Analysis

After scheduling, observing, correlation, and fringe-fitting have been done, the data volume has decreased from hundreds of terabytes to several tens of megabytes. The raw observations of the noise of the quasars have been reduced to the observed (group) time delays between telescopes.

In the analysis step the time delays are used to estimate the eventual parameters of interest such as the EOPs, station (i.e. telescope) positions, and/or quasar positions. For this specialized programs are used, such as, for example *C5++* (Hobiger et al., 2010), primarily used in this thesis for the analyses performed, and *VieVS* (Böhm et al., 2018).

In the next two sections the general steps needed to go from time delays to parameters and the time delay modeling are discussed.

3.4.1 From time delays to parameters

In order to go from the observed time delays to estimating the wanted parameters, one needs to understand that the time delays from the observations are *observed* time delays, and not the actual pure geometric time delays between to two telescopes. So, to get the actual geometric delay, which we can then use to determine parameters of interest such as EOPs and station positions, we need to determine or estimate the time delays caused by other effects that are on top of the geometric time delay. A representation of this per observation is:

$$\tau_{obs} = \underbrace{\tau_{geom} + \tau_{rel}}_{\text{consensus model}} + \tau_{clk} + \tau_{tro} + \tau_{ion} + \tau_{inst} + \tau_{source} + \epsilon \qquad (3.2)$$

Here τ_{obs} is the actual observed time delay from the experiment, τ_{geom} is the geometric time delay which is a function of the station positions in the Geocentric Celestial Reference System (GCRS) and the telescope deformations, τ_{rel} is the time delay caused by relativistic effects, τ_{clk} is the time delay introduced by offsets and drifts of the atomic clocks at each of the two stations, τ_{tro} is the delay caused by the dry and wet parts of the tropopshere at each of the telescopes, τ_{ion} is the delay caused by the ionosphere (which is already solved for in the fringe fitting process for VGOS), τ_{inst} are station specific instrumental time delays such as cable delays, τ_{source} is the time delay caused by offsets in the source (quasar) position or radio emission location, and finally ϵ is a residual error due to unmodeled time delays.

The first two time delays on the right hand side of the equation are grouped and denoted as the *consensus model*. This is the name for a model that is adopted in the IERS 2010 conventions for VLBI analysis, which combines both these time delay contributions in one consistent model (Petit and Luzum, 2010). This model essentially connects the baseline observation of the quasar in ICRS to the station positions in the ITRS using the EOPs, taking into account relativistic effects.

We can see from Equation (3.2) that we need to determine several time delays on the right hand side, which we can then subtract from the observed time delay τ_{obs}, in order to solve the consensus model and find the parameters

of interest. The time delays which are typically not of primary interest are called nuisance parameters. If we would not solve for these, we would solve the consensus model with all these time delays included and would not achieve an accurate solution from the consensus model.

The nuisance parameters are estimated using models of which the values are estimated together with the solving of the consensus model by using a Markov-Gauss least squares approach, although Kalman filters can and have been used as well. This approach tries to minimize the so called O minus C (O-C) vector using least squares. In Equation (3.2) the left side of the equation is the observation (O) part and the right side the computed (C) part. If O-C is exactly zero we have modeled all the delays correctly; this is however unlikely, but it is possible to minimize the overall residuals of all the combined O-C values of all the observations in a session. Usually, this method requires an iterative approach in which the solution slowly converges to the minimum, due to the non-linearity of the problem. In each iteration the models are recalculated using the estimated parameters which are adjusted by the least squares adjustment.

For some modeled parameters it is necessary to set constraints, to avoid that the solution diverges or includes unrealistic modeling outcomes. For example, the troposphere delay is expected to only change a limited amount from hour to hour, and station positions are not expected to deviate too much from their apriori values. Often used constraints are rate constraints, limiting the change of the parameters over time, commonly used for the troposphere and clock parameters, and no net translation (NNT) and no net rotation (NNR) constraints which limit the station network's global movement in the estimation.

In the end the estimated solution contains typically, for example for a 24 hour session with more than 6 telescopes, six station positions in x, y, and z in the ITRF and five EOPs from the *consensus model*, 2nd degree polynomials for the clocks of each station from τ_{clk}, and about three wet troposphere parameters per hour per station from τ_{tro}. Meanwhile, τ_{ion}, τ_{inst} and τ_{source} are typically not estimated, because for VGOS τ_{ion} is already solved for in the fringe fitting process (and is thus not included in the τ_{obs}), τ_{inst} is taken from the database, and τ_{source} is mainly only estimated specifically for ICRF solutions.

A more in-depth discussion on the time delay modeling is given in the next Section.

3.4.2 Time delay modeling

To do the least squares adjustment in the analysis, every part of the computed time delay has to be modeled, estimated, or accounted for in some way. In the following sections each time delay in Equation (3.2) will be discussed.

3.4.2.1 The consensus model

The consensus model encompasses both the geometric delay τ_{geom} and the relativistic delay τ_{rel}.

The relativistic delay τ_{rel} is made up of several components which leads to delays and bending of the signal and include: the effect of the geocentric reference frame moving around the Sun and gravitational effects of the Earth, Moon, Sun and other planets which cause the signal to bend in space-time.

At the base of the geometric delay τ_{geom} is the following relation:

$$\tau_{1,2}(t) = -\frac{1}{c} \cdot \vec{b} \cdot \vec{k} \tag{3.3}$$

where $\tau_{1,2}$ is the time delay between the two telescopes, c is the speed of light, $\vec{b}$ is the baseline vector between the two telescopes and $\vec{k}$ is the unit vector pointing toward the quasar, both defined in the GCRS. Since the baseline vector $\vec{b}$ is given in the GCRS, it means that the input station positions in the (Earth fixed) ITRS first need to be transformed using the EOPs to the (non-Earth fixed) GCRS using Equation (3.4).

$$\underbrace{X_{GCRS}}_{\text{Inertial}} = \overbrace{Q_{X,Y}}^{\text{Celestial pole}} \cdot \underbrace{R_{ERA}}_{\text{Earth rotation}} \cdot \overbrace{W_{xp,yp}}^{\text{Polar Motion}} \cdot \underbrace{X_{ITRS}}_{\text{Terrestrial}} \tag{3.4}$$

In this Equation X is the station position, or a baseline $\vec{b}$, in cartesian x, y, and z coordinates in the GCRF or the ITRS, $Q_{X,Y}$ represents the transformation matrix related to the celestial pole offsets in x and y, R_{ERA} the transformation matrix related to the Earth rotation angle, and $W_{xp,yp}$ the transformation matrix related to the polar motion.

The consensus model supplies the geocentric vacuum delay $\tau_{2,1}$ for the baseline between station 2 and 1, taking into account the pure geometric and relativistic (or gravitational) delays as:

$$\tau_{2,1} = \frac{\Delta T_{grav} - \frac{\vec{k}\cdot\vec{b}}{c}\left[1 - \frac{(1+\gamma)U}{c^2} - \frac{|\vec{V}_E|^2}{2c^2} - \frac{\vec{V}_E\cdot\vec{\omega}_2}{c^2}\right] - \frac{\vec{V}_E\cdot\vec{b}}{c^2}(1 + \vec{k}\cdot\frac{\vec{V}_E}{2c})}{1 + \frac{\vec{k}\cdot(\vec{V}_E+\vec{\omega}_2)}{c}} \tag{3.5}$$

Which is documented in (Petit and Luzum, 2010) where also an in-depth description of all variables can be found.

The baseline vector $\vec{b}$ in Equation (3.5) should be as accurate as possible, so the station positions used from the ITRF should have additional geophysical effects added through the use of models. Below, a brief summary is given of all these added geophysical models.

Solid Earth tides The solid Earth tides are tides caused by the Sun and Moon causing gradual periodic rise and fall of the solid Earth's surface of about a meter (Wahr, 1981).

Ocean tide loading The ocean tide loading causes displacements of the solid Earth's surface due to the weight of the oceans, which change due to ocean tides caused by the Moon and Sun, and are typically on the order of several centimeters (Scherneck et al., 2000; Sovers, 1994).

Pole tide loading Pole tide loading is the response of the solid Earth's surface and oceans to the centrifugal force induced by polar motion. The vertical displacement caused by the solid pole tide loading is typically on the order of 2 cm, and for the ocean pole tide loading is typically just a few mm (Desai, 2002; Gross and Vondrák, 1999).

Tidal atmospheric loading Tidal atmospheric loading is the response of the solid Earth's surface to periodic changes in atmospheric pressure and mass due to, among others, the day-night cycle heating by the Sun, the gravity of the Moon, and deep convective processes in the tropics. The effect is on the order of a few millimeters to few centimeters (Haas et al., 1997)

Post-seismic deformations The ITRF solutions of the station positions also include a velocity component which does include the motion of the stations due to plate tectonics and glacial isostratic adjustment (GIA). The ITRF solutions also include discontinuities caused by earthquakes, which means the position and velocity timeseries gets split into separate parts between earthquakes to account for the abrupt station position changes. Due to the elasticity of the Earth's crust, directly after an earthquake the position and velocity of a station shows some non-linear behavior that needs to be taken into account and is given in the ITRF solution's accompanying post-seismic deformation file.

Thermal and gravitational deformations Although this is more relevant for the legacy VLBI system, the thermal and gravitational deformations of the telescopes need to be taken into account. The thermal deformation is caused by changes in the ambient temperature around the telescope that causes the telescope to deform. This can be both for the whole vertical structure, causing a change primarily in the up component of the telescope, as well as for the telescope reflector, which may change shape due to stresses in the material heating up or cooling down causing the signal path length to become longer or shorter. Meanwhile, the gravitational deformation is primarily caused by the reflector of the telescope deforming under its own weight, which causes changes in the signal path length. Both these effects are of different magnitudes for the Legacy and VGOS system, where for the Legacy system it can be on the order of centimeters and for VGOS it usually is less than 1 cm (Nothnagel, 2009).

Telescope axis offsets For older telescopes the primary and secondary axes may not intersect causing an axis offset that needs to be taken into account because the error can be on the order of centimeters (Nilsson et al., 2017). For VGOS this effect is negligible.

3.4.2.2 The clock delay

Even though Hydrogen-masers used at VLBI stations, to time tag the measurements, have a stability of about 1×10^{-14} s/s their drift is noticeable and needs to be accounted for. In the analysis, one station is kept as the reference and the others have their drifts and offsets modeled. Usually, for each modeled clock a

2nd degree polynomial is estimated over the course of the whole experiment with hourly or half-hourly piece wise linear offsets with constraints applied to keep the offsets within a realistic range.

3.4.2.3 The troposphere delay

The troposphere delay can be split up into two components: the dry and wet parts of the troposphere. The wet part of the troposphere has a considerable effect on the time delay and is on the order of a few decimeters.

The dry part of the troposphere is usually well modeled (Saastamoinen, 1972), however the wet part of the troposphere, mainly caused by water vapor in the atmosphere, is very variable and has to be estimated. The estimation of the troposphere usually has 3 variables at any given time: one is the Zenith Wet Delay (ZWD) which is the best fit of all the wet troposphere delays mapped using a mapping function based on the elevation of each observation, and two related to the north and east gradients (NGR, EGR) of the wet delay. The ZWD is a constant value for a telescope over some chosen time span that is mapped to every observation with some elevation dependent mapping function. A mapping function can be one such as the global mapping function (Boehm et al., 2006) or a Vienna mapping function (Landskron and Böhm, 2018). The gradients in the north and east directions are estimated to capture the variability of the mapped wet delays in two orthogonal azimuth directions.

The magnitude of the ZWD and the gradients is roughly tens of centimeters and a few millimeter respectively (Sovers et al., 1998).

3.4.2.4 The ionospheric delay

The ionospheric delay can be well estimated if at least two measurements are done at different frequencies. This is done for the legacy system, but as mentioned, this has already been taken care of in the fringe fitting process for VGOS. The magnitude of the delay caused by the ionosphere is on the order of a tens of centimeters (Sovers et al., 1998).

3.4.2.5 The instrumental delay

Instrumental delays can not be estimated and are included in the databases. Instrumental delays can for example be the cable cal value that is included in the database to account for the length of cables between the telescope and the backend which does the time tagging, which is usually on the order of a few hundred picoseconds (García-Carreño et al., 2022), thus can be equal to about 10 centimeters.

3.4.2.6 The source induced delays

There are different delays caused by the observed quasars: delays caused by the wrong apriori position of the quasar, delays caused by source structure, and delays caused by the source position being different in different frequency bands.

The magnitude of these delays differs a lot. Apriori quasar position changes are rare, but can cause errors, together with source position being different in different frequency bands, of a few tens of picoseconds (Xu and Charlot, 2025; Xu et al., 2022), depending on the offset (roughly 10 ps per 0.1 mas offset). Depending on what source structure is present, extended or not, the effect can be several hundred or a few tens of picoseconds (Charlot, 1990; Xu et al., 2016; Xu et al., 2021a).

3.4.2.7 Near-field delay models

If instead of quasars in the far field, satellites or other radio sources would be observed in the near field, different models for the geometric and relativistic delays should be used. The assumption that the radio emission arrives at the telescopes as a plane wave, and that the radio sources are stationary within the ICRS does not hold up in that case. In that case a near field delay model should be used instead of the consensus model from the IERS conventions.

Different near field delay models have been developed in the past decades (Duev et al., 2012; Jaron and Nothnagel, 2019; Klioner, 1991; Sekido and Fukushima, 2006), which all have slight differences in terms of being numerical or analytical and in terms of in which reference frame the delays are calculated. So far, the found performance differences in terms of accuracy and precision between all the near field delay models have been far below the 1 ps level (Jaron and Nothnagel, 2019; Schunck et al., 2026, March) and therefore no preference has been given to any of these models, except for the fact that the analytical models are more stable and faster in execution. Selected VLBI analysis software packages have near field delay models implemented (Böhm et al., 2018; Klopotek et al., 2017) and can in theory be used to analyze VLBI observations of radio sources, such as satellites and rovers, in the near field. As of writing no IERS convention regarding the use of near field delay models exists.

3.5 Simulations

Simulations are an effective way of assessing the performance of future scenarios in case that no real observations are available. Within the VLBI field simulations are used to assess the performance of generated observation schedules for VLBI ahead of the actual experiment and can help in the further optimization of such schedules by assessing multiple schedules with different optimization criteria (Schartner and Böhm, 2019). Furthermore, VLBI simulations have been used in the design of the VGOS system (Pany et al., 2011), for the assessment of optimal placement locations for telescopes (Schartner et al., 2021), for assessing scheduling optimizations (Gipson and Baver, 2015; Gipson and Baver, 2016), in case studies of observing lunar rovers on the surface of the Moon using VLBI (Klopotek et al., 2018), and in studies related to geodetic VLBI observations of Earth orbiting satellites (Klopotek et al., 2020; Schunck et al., 2024; Wolf et al., 2025).

In geodetic VLBI simulations, the group delays are usually simulated by taking the geometric and relativistic delay in the far-field or near-field, from the consensus model or a near field delay model, to which simulated nuisance parameter influences are added. The nuisance parameters, also called error sources, that are usually simulated are (wet) tropospheric turbulence, clock instabilities, and random measurement noise. A simulated delay τ_{sim} on a baseline can be expressed as

$$\tau_{sim} = \tau_{2,1} + (\tau_{trop2} + \tau_{clk2}) - (\tau_{trop1} + \tau_{clk1}) + \tau_{meas} \tag{3.6}$$

Here the simulated delay τ_{sim} is thus the sum of the geometric and relativistic delay $\tau_{2,1}$, the delays due to tropospheric turbulence τ_{trop2} and clock instabilities τ_{clk2} at station 2, the delays due to tropospheric turbulence τ_{trop1} and clock instabilities τ_{clk1} at station 1, and the measurement noise on the observation τ_{meas}.

The simulated delay is in practice computed as

$$\tau_{sim} = \tau_{2,1} + (ZWD_2 \cdot m_w(\epsilon_2) + clk_2) - (ZWD_1 \cdot m_w(\epsilon_1) + clk_1) + \tau_{meas} \tag{3.7}$$

Where the tropospheric turbulence induced delay τ_{trop} per station is modeled through the simulated turbulence's ZWD per station mapped with a (wet) mapping function m_w to the elevation ϵ of the observation and is usually based on the work by Nilsson and Haas (2010). The delay due to the instabilities of each clock clk is usually modeled as the sum of random walk and integrated random walk processes as described by Herring et al. (1990). The measurement noise is modeled as a gaussian white noise process.

Parameterization for these 3 error sources is rather standard (Klopotek et al., 2020; Pany et al., 2011). The troposphere is usually parameterized using a refractive index structure constant C_n, wind velocity v, atmospheric scale height h, number of layers n, and a base ZWD have to be chosen for the simulations. The C_n value is usually taken around $1.8{\times}10^{-7}$ $\mathrm{m}^{-1/3}$, the velocity around 8 m/s, scale height of 2000 m, either 10 or 20 layers and a ZWD of around 0.15 m. The clocks are modeled using a Van Allan standard deviation of $1{\times}10^{-14}$ s/s over 50 minutes. The measurement noise it depends on which system is simulated, where for Legacy it is usually taken around 30 ps (Pany et al., 2011) and for VGOS around 2-5 ps for quasars (Nilsson, 2022; Xu et al., 2022) and 10 ps for satellite observations (Kern et al., 2026; Wolf et al., 2025).

To simulate a whole session of group delays a schedule file can be taken for which each observation is then simulated. After the simulated delays have been written to a database, such as NGS, a VLBI analysis program can be used to analyze the database.

In order to get a proper statistical analysis of the simulated scenario a Monte Carlo approach should be used (Klopotek et al., 2020; Pany et al., 2011), since the simulations are based on random simulated processes. In this approach the simulation and subsequent analysis are carried out multiple times. This ensures that the overall analysis includes a large amount of combinations of the simulated random processes and a good overall assessment of the performance can be made.

Furthermore, this method allows us to find the accuracy and precision of the parameters since the true input parameters are know, such as the supplied EOPs and station positions.

3.6 Simulation validation

Though simulations are used widely for VLBI and their usual parameterization is widely accepted, their validation might be considered underexposed. Studies have compared simulation results with real results (Nilsson and Haas, 2010; Nilsson, 2022; Schartner, 2025), and in most cases confirmed simulations to be too optimistic.

Recent work has tried to make simulations more accurate by focusing on determining global realistic C_n and v values based on machine learning models and GNSS data (Schartner, 2025). This should allow for a more realistic turbulent troposphere simulation. Though the method employed seems reasonable, the derived C_n values are rather high compared to earlier work (Nilsson and Haas, 2010) and the common constant value used for C_n of $1.8{\times}10^{-7}$ $\mathrm{m}^{-1/3}$.

In the light of the Genesis mission, for which a lot of research is dependent on simulations, a reassessment of the state of the art of VLBI, and particular VGOS, simulations is beneficial.

A study into the realism of simulated VGOS 24 hour sessions has been done and presented at a conference, but not included or appended in this thesis. The preliminary conclusions were that, in terms of troposphere turbulence simulation, the recent C_n values as published by Schartner (2025) produced too high residuals, that the commonly used constant standard value of $1.8{\times}10^{-7}$ $\mathrm{m}^{-1/3}$ for C_n is reasonably ok, but does not capture seasonality, and that per site daily derived C_n values based on co-located GNSS stations produces the most realistic results. Additionally, daily VGOS session derived C_n values produced similar results as the daily co-located GNSS derived values, but the per VGOS session derived values produced rather chaotic results. Furthermore, a discrepancy in the station positions over longer timescales was found, and the hypothesis is that it has to do with the mismodeling of the station positions. Work like this could potentially also be used to inversely determine error sources contributions in VGOS. This work is planned to be continued to enable for more realistic simulations.

Overall, more research should be done to ensure that simulations produce realistic results.

Chapter 4

Radio sources in VLBI

Author note: This chapter is the main part of the thesis; It gives an overview of present challenges in the observations of quasars and satellites for VGOS. It sets the stage for paper I on source structure informed scheduling for VGOS intensive sessions (in review) and the research being done for the upcoming Genesis mission (unpublished).

As explained before geodetic VLBI uses far away radio sources to determine delays between telescopes. These radio sources are in almost all cases quasars (described in Section 4.1.1), which can be used very well to determine EOPs and the ITRF. Still, even though quasars have always been part of geodetic VLBI, they themselves still introduce errors in the group delay modeling. Moreover, with the advances of VGOS some difficulties arise due to the different frequencies used compared to the legacy S/X system. In Section 4.1.2 an in-depth overview is given on these quasar related challenges for VGOS.

More recently, the geodetic VLBI community explored the possibility of observing artificial radio sources, such as satellites, rovers, and stationary emitters on the Moon. Such observations can aid in the determination of satellite orbits, find intra-technique biases, aid Selenodesy, and support navigation platforms, for example, around the Moon. In Section 4.2 the observation of satellites, and in particular Genesis, is discussed further, and challenges related to it are highlighted.

4.1 Quasars

Quasars are the main observed radio sources in geodetic VLBI, but what are quasars? Why are they chosen to be observed? And what are their unwanted effects on the geodetic observables? These questions are answered in the next sections.

4.1.1 What is a quasar?

Quasar stands for quasi stellar radio source and stems from a time when the astronomical observations were not able to distinguish what these kind of bright

radio emitting star-like objects were. The first quasar 3C273 was observed and documented by Schmidt (1963). This finding was published in an article named "A Star-Like Object with Large Red-Shift", which highlights the belief back then that these were star-like objects. In the narrow radio spectrum they seemed to be point-like like stars, but were in most cases not visible in the visible light spectrum. Since they looked like stars in a sense and emitted in the radio frequency band, they were called quasi stellar radio objects.

By now we know they are Active Galactic Nuclei (AGN) (Blandford et al., 2019), actively accreting black holes in the center of other galaxies (spirally or elliptical systems of primarily stars, gas, and dust), just like the one in the center of our Milky Way called Sagittarius A*. The fact that these black holes are actively accreting material generates a lot of energy in the accretion disk, as well as two enormous relativistic (close to speed of light) jets perpendicular to their galaxy's rotational plane or disk. Especially these jets emit high amounts of radio emissions as synchrotron radiation, the radiation emitted by electrons spiraling in strong magnetic field lines. The jets themselves are highly collimated and consist of charged particles that are accelerated through the magnetic field lines, which guide those jets.

The fact that these black holes appeared stellar was simply because of the angular resolution of the radio telescopes used back in the day. Especially with the advance of VLBI in astronomy it became clear that these stellar looking sources were not stellar at all. The fact that they looked pointlike, even though they are gigantic galaxies, is due to the fact that these objects are at astronomical distances (and thus time) away from us, at cosmological origin. It is now known that quasars are at redshifts between 0.15 and 10, which means at distances of a 2 - 3 billion to about 12 - 13 billion light years away (just as a reference the universe is estimated to be 13.8 billion years old). At high redshifts the universe is relatively young (the radiation takes billions of years to reach us) and most of the quasar's electromagnetic radiation has been highly red-shifted, due to the expansion of the universe, into the radio regime.

4.1.2 Quasar effects in VGOS

Even though quasars are very far away and their emission can be assumed to be a plane wave when reaching Earth, their actual structure can be resolved with VLBI on intercontinental baselines (Charlot, 1990). This source structure is mostly visible when observing quasars where their jets are visible and show observable movement in monthly or yearly timescales (Kostrichkin et al., 2025). Their observed structuredness can be categorized using so called source structure indices (SI) (Fey and Charlot, 1997), which are typically values from 1 to 4 with increasing values meaning more observed source structure. In geodetic VLBI only quasars that show a low amount of source structure (typically SI $\leq$2) are considered good and should primarily be observed (Fey and Charlot, 1997), because the effect influences the apparent (and in the analysis assumed apriori) position of the quasar.

Two different effects related to source structure affect the geodetic analysis primarily (Xu and Charlot, 2025). Firstly, source structure can cause the

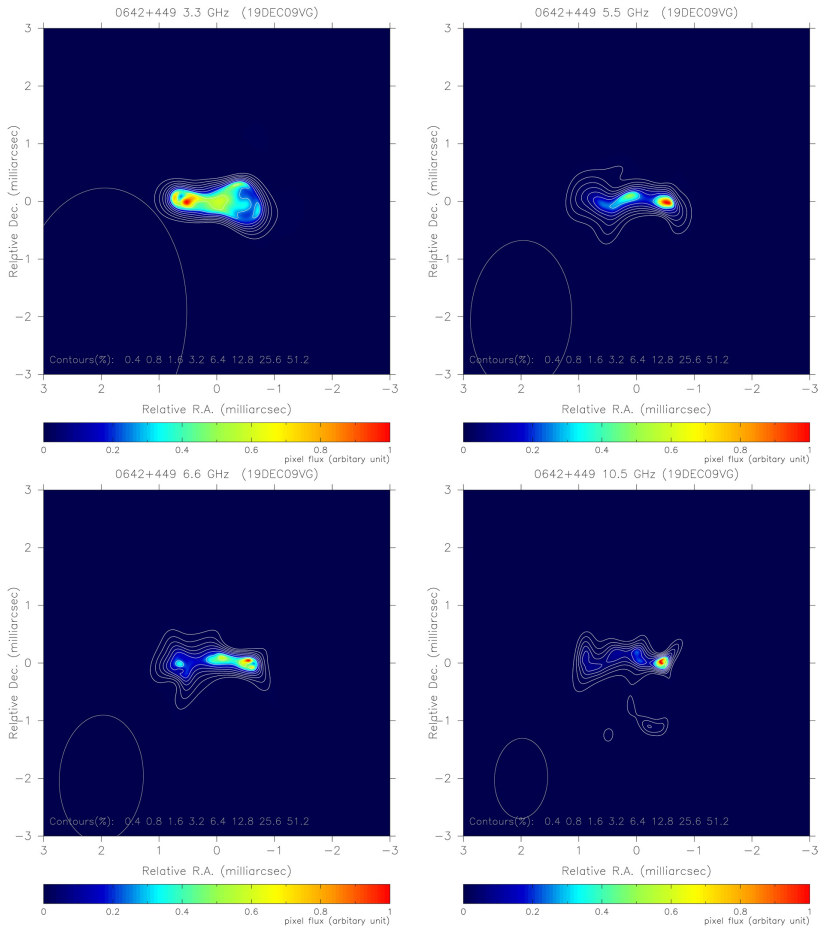

Figure 4.1. Images of source 0642 + 449 at the frequencies of 3.3, 5.5, 6.6, and 10.5 GHz from VGOS observations VT9343. Credit: Xu et al. (2021c).

astrometric position of the radio emission center, the brightest radio emission point, to move along the jet (Gattano and Charlot, 2021), and thus changes its assumed source position (Xu et al., 2022). Secondly, the radio emission center is located at different astrometric positions in different frequencies due to the quasar jet's opaqueness at different frequencies (Xu et al., 2021b; Xu et al., 2021c; Xu et al., 2022), see for example Figure 4.1. These two effects related to source structure can cause residuals in the analysis on the order of several to hundreds of picoseconds.

The movement of the radio emission along, or with, the jet can cause residuals of about tens of picoseconds (see Paper I in Section 5.1.1). These effects are baseline length and baseline orientation dependent. A baseline is, in terms of orientation, primarily sensitive to movement of the radio emission of the source in the uv-plane, referring to the 2D projection in the sky plane (see Figure 4.2), parallel to the projection of that baseline onto the uv-plane

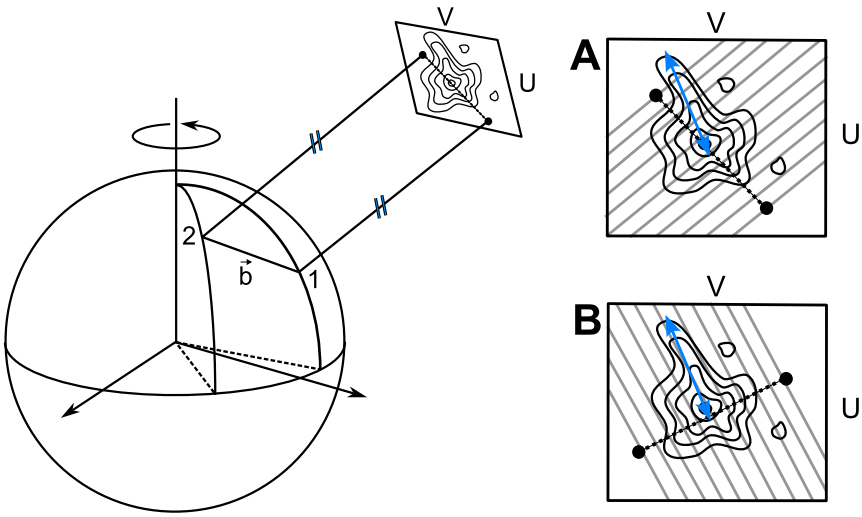

Figure 4.2. *left* The baseline $\vec{b}$ projected onto the uv-plane of the observed quasar, equal to case A. *right* Different projected baseline cases with a potential baseline interference pattern indicated by grey lines and the jet indicated by the blue arrow. **A:** The jet and projected baseline are almost aligned, the baseline is sensitive to the potential movement of the radio emission along the jet. **B:** The jet and projected baseline are almost perpendicular, the baseline is not sensitive to the potential movement of the radio emission along the jet.

(Charlot, 1990; Shabala et al., 2015; Xu et al., 2016). The delays observed by a baseline of a stable and steady radio source should be the same along these parallel lines in the uv-plane, which corresponds to the potential interference pattern of that observation (Plank et al., 2016). In Figure 4.3 an image of the structure (i.e. the brightness distribution) of source 0812+367 is shown and in Figure 4.4 the visibilities of source 0812+367, both taken from the Bordeaux VLBI Image Database (BVID)[1]. Notice that in the direction perpendicular to the jet of the quasar the measured visibilities, which is also related to the delay, change less than in the parallel direction.

The movement of the actual radio emission w.r.t the assumed apriori position can cause residuals on the order of several hundreds of picoseconds if the source has multiple components (Xu et al., 2016). For the error due to two component source structure, the length of the baseline also plays a role. If all angles between the source jet direction (or primarily movement) and the projected baseline onto the uv-plane are observed (lets call that angle α), for example by a northern hemisphere baseline towards a source at high declination over the course of 24 hours, one would typically see a peak in residuals when those two are in parallel when $\alpha = 90$ degree or $\alpha = 270$ degree (Xu et al., 2016). However, depending on the baseline length and the distance between the two source components, longer baselines may start to observe two peaks

[1]Bordeaux VLBI Image Database (BVID). This database can be reached at https://bvid.astrophy.u-bordeaux.fr/

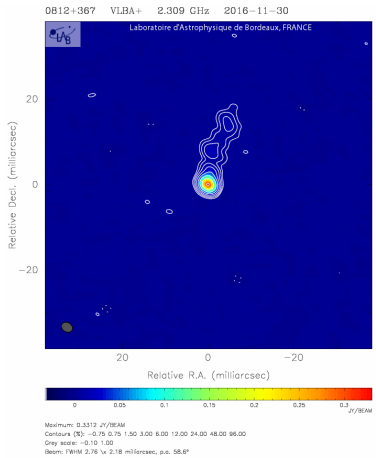

Figure 4.3. An VLBI image of radio source 0812+367, from BVID.

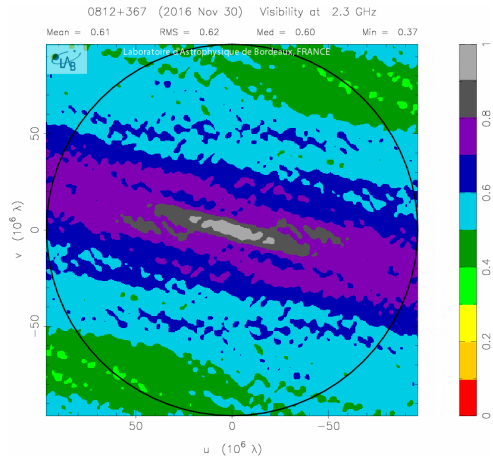

Figure 4.4. A visibility map of radio source 0812+367, from BVID.

centered around the 90 and 270 degree α angles. This happens because at certain baseline lengths the angular resolution becomes good enough to observe only one of the source components when $\alpha = 90$ or 270 degree, but cannot distinguish the components when they are closer together on the projected baseline at slight deviations from the 90 or 270 degree angles.

The influence of the different frequencies used in VGOS accounts for errors on the order of tens of picoseconds. The actual error depends greatly on the position offsets in the different frequency bands, but it is estimated that on a 9000 km baseline an offset in one of the bands of 0.2 mas can lead to an extra delay of about 30 ps in one band. This single band delay can propagate to the broadband delay and cause a factor two times higher delays (Xu et al., 2022).

If the aim is to produce reference frames on the order of 1 mm accuracy ($\approx$ 3 ps) these errors should be better understood and mitigated. In the legacy S/X system the source structure effect was estimated to be around 40 % of the error budget (Anderson and Xu, 2018). Different ideas have been proposed to reduce the source structure induced residuals. For example, one can try removing source structure in DiFX visibility data (Jaron et al., 2025), or one can re-weight observations based on the α-angle (Kareinen et al., 2024), or one can try to mitigate its effect completely by observing quasars in such a way that the movement of the radio emission center is perpendicular to a baseline, in which case that movement should have no effect on the observation (see Paper I in Section 5.1.1).

Despite all these efforts it still is a topic of ongoing research.

4.2 Satellites

Man made satellites have become essential for society by contributing, among others, to communication, planetary science (including Earth itself), engin-

eering, science, our understanding of the universe, and navigation. Without them, weather prediction, climate change and sea level monitoring, remote communication, and global (phone) navigation would not be possible (Pelton et al., 2017).

Satellites are typically spacecraft that serve a specific purpose and are launched, using a rocket, into an orbit that aligns with their objective. Usually they are designed and built around their main instrument (called payload), for example, a camera to observe the Earth, which sets requirements on their orbit, lifetime, thermal conditions, power usage and generation, attitude determination and control systems, data storage and handling, and the like (Wertz et al., 1999). Typical sizes of spacecraft are between as small as a milk carton or as large as a school bus, and their weights can be from hundreds of grams to many tons. In the end, usually, the data gathered by the spacecraft is what makes a satellite mission worthwhile.

Not only data generated on board satellites are of use, but also the satellites themselves. Satellites form an interesting observable artificial radio source for determining frame ties between different geodetic techniques (Bar-Sever et al., 2009; Biancale et al., 2017; Delva et al., 2023; Rizos and Willis, 2014); they are in general well observable and available in comparison to local Earthbound methods. Some Earth observation satellites already have 3 of the 4 space geodetic techniques onboard, such as Sentinel-3A (Montenbruck et al., 2018), to aid in the orbit determination of the satellites, but limited work has been done on determining frame ties using these satellites. Furthermore, VLBI has been the only absent technique on them.

The lack of VLBI onboard satellites is due to multiple reasons, but the two most important ones are that, firstly, VGOS is not inherently designed to be used to observe satellites, and in order to achieve good (quasar like) performance a rather complicated VLBI signal transmitter would need to be designed, and secondly, that most Earth observation satellites orbit at relatively low altitudes below 1000 km, which means not a lot of VLBI telescopes would be able to observe such satellites at the same time. The upcoming Genesis mission from ESA will change this and aims to put a satellite in a 6000 km altitude orbit which is observable with all four space geodetic techniques.

In the rest of this chapter an overview is given of satellites orbits, precise orbit determination, satellite observations with VGOS, and more on the Genesis mission and its challenges.

4.2.1 Satellite orbits

Orbits are descriptions of how the center of mass of an object, a satellite, moves through a space influenced by gravity and other forces. In astronomy this topic is usually called celestial mechanics, whilst in spaceflight this is called astrodynamics or orbital mechanics. A lot of excellent books can be found on satellite orbits (Montenbruck et al., 2002; Vallado, 2001; Wakker, 2015; Wertz, 2001), but this chapter only gives a basic summary.

Once a satellite has been successfully launched, it is usually orbiting around an object it is gravitationally bound to. In case of Earth orbiting satellites,

the main body it orbits around will be Earth, but depending on the mission it can also orbit around the Moon, another planet, an astroid, and even the Sun, as long as it is the main gravitational attractor in that space. Satellites can also have such a high velocity that they overcome their gravitationally bound object and escape it, allowing the transfer to other bodies or the escape the solar system in its totality.

A satellite stays "in orbit" because its velocity is large enough and in a direction that is close to perpendicular to the pull of the main body it orbits around. In essence, the satellite goes forward fast enough that the pull of the main body below, which depends on the distance between the two, only curves the trajectory. If the combination of these variables is within a certain bound, the satellites will be orbiting the main body and will neither crash into it nor escape it. Thus, in launching a satellite, the aim is not just to get the satellite at a high enough altitude but also at a high enough velocity in the desired direction.

An object in orbit adheres to Kepler's 3 laws of planetary motion which dictate that, in simple form, (1) all bound orbits are ellipses, (2) there is a relation between the amount of orbit traversed and time passed, and (3) the relation between the orbit size and the orbital period (Wakker, 2015). These laws are still correct today and are the basis of celestial mechanics.

Another core principle of orbital motion is Newton's law of universal gravitation (Wakker, 2015), which can be written as

$$F = G\frac{m_1 m_2}{r^2} \tag{4.1}$$

which states that the force F applied to two bodies close to each other is a function of the gravitational constant G, the masses of the bodies m_1 and m_2, and the distance between the two bodies r.

Under the assumption that one of the two bodies is much heavier than the other (in the case of Earth $m_1 = M$ and a satellite $m_2 = m$), that $\vec{u} = \vec{r}/r$ (to allow vectorization), and that $F = m \cdot a$ we can rewrite the equation to get the acceleration acting on the satellite, ignore the acceleration on the Earth, as e.g.

$$\vec{a} = \frac{d^2\vec{r}}{dt^2} = -G\frac{M}{r^3}\vec{r} \tag{4.2}$$

This shows that based on the distance from the main body the satellite gets accelerated towards the main body ($\vec{r}$ is defined from the main body to the satellite). This equation is also at the core of dynamic orbit determination, discussed further in Section 4.2.2, albeit it will need some more added accelerations. Together with the earlier mentioned typically large (almost) perpendicular velocity of a satellite w.r.t. this acceleration vector, the velocity vector gets bent towards the main attractor, by $\vec{r}_{n+1} = \vec{r}_n + \vec{a}_n \cdot t$, and at every point in time curves around the main attractor. This is the basis of the physics behind orbital motion.

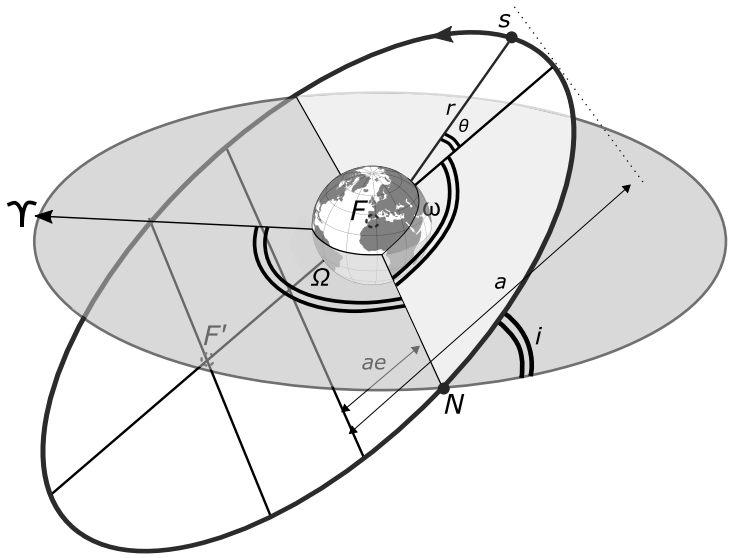

Figure 4.5. A 3D view of the orbital plane with the two focal points of the ellipse (F and F'), the satellite S at radius r, the semi-major axis a, the eccentricity e, the true anomaly θ, as well as the angles that indicate the orientation of the plane in 3D space using the inclination i, the right ascension of the ascending node (N) Ω, and the argument of perigee ω. The vernal equinox is denoted with Υ and the equatorial plane is colored gray.

Orbit descriptions

To represent an orbit in 3D space around a main body, different representations exist. Most commonly the classical orbital elements are used (Montenbruck et al., 2002) (See Figure 4.5). To describe the shape of the orbit two elements are used: the semi-major axis a which describes the size of the orbit, and the eccentricity e describing the orbit's ellipticity. In order to know where the satellite is in this ellipse the true anomaly θ is used; it describes how far in the orbit the object is from the perigee. The perigee the closest point in the elliptical orbit to the main attractor and the apogee the furthest. Three angles are commonly employed to describe to orientation of orbital plane and the perigee in 3D space: the inclination i describing the tilt of the orbital plane w.r.t the equatorial plane, the argument of right ascension of the ascending node (RAAN) Ω describing the angle of the crossing point (ascending node N) from the southern hemisphere to the northern hemisphere w.r.t the vernal equinox Υ (A fixed direction in space), and the argument of perigee ω describing how many degrees in the orbital plane the perigee is located.

For circular orbits the eccentricity e is zero and the perigee and apogee are undefined (and thus also the argument of perigee ω). For equatorial orbits the inclination is zero and the RAAN Ω and argument of perigee ω are in principle undefined. To overcome such difficulties, different non-singular orbital elements can be used which are commonly referred to as non-singular, regular

or equinoctial elements (Montenbruck et al., 2002).

In general orbits can be represented differently, but always will include at least 6 parameters, as for the 6 classical orbital elements. Especially when describing orbital motion in a numerical way the orbital element might not be the most handy option, and thus often, in orbit determination and orbit prediction the representation of a satellite orbit is done using a position vector and an accompanying velocity vector, which together are called a state vector.

Orbit descriptions, data, and formats that are also commonly used are Standard Product 3 (SP3)[2], Two-line elements (TLE) (Vallado et al., 2006), and Consolidated Prediction Format (CPF)[3].

Orbit propagation

An orbit is called a Keplerian orbit in case no perturbations (perturbing forces) are acting on it, meaning only the main body exerts its gravitational pull as a point mass on the satellite (Wakker, 2015). These orbits are inert and have only limited applicability in real life applications such as orbit determination (what is the orbit given a set of observations) and orbit propagation (the prediction of the orbit state further in time). Therefore, perturbations are usually taken into account.

Perturbations are gravitational and non-gravitational forces, other than the zeroth order gravitational pull, acting on the satellite, such as higher order spherical harmonics of the gravity field (ideally including solid Earth, oceans, and atmosphere), atmospheric drag, solar radiation pressure (SRP), 3rd body perturbations (pull of Sun, Moon, and other planets), planetary albedo, planetary infrared radiation, and possible maneuvers. For an overview of the order of magnitude of each of these perturbations, see Montenbruck et al. (2002, Fig. 3.1). These perturbing forces are very important because their influence constantly change the orbital parameters.

Lets take a look again at the earlier acceleration Equation (4.2), but now with some added perturbations (also called Cowell's method)

$$\vec{a} = \frac{d^2\vec{r}}{dt^2} = -G\frac{M}{r^3}\vec{r} + \vec{a}_{drag} + \vec{a}_{SRP} + \vec{a}_{grav} + \vec{a}(...) \tag{4.3}$$

Here, accelerations acting on the satellite are added, such as for air drag, solar radiation pressure, the spherical harmonic gravity field, and $\vec{a}(...)$ being all other unnamed acceleration.

What is important to note is that most perturbations act in different directions on the satellite (Montenbruck et al., 2002). While the first term, from the zeroth order gravitational pull of the main body, acts towards the center of the main body, the other accelerations do not. The air drag per definition acts opposite to the direction of travel, the solar radiation pressure acts opposite to where the Sun is, and the spherical harmonic gravity field

[2]The Extended Standard Product 3 Orbit Format (SP3-d) by S. Hilla, https://files.igs.org/pub/data/format/sp3d.pdf

[3]Consolidated Prediction Format (CPF) at the ILRS, https://ilrs.gsfc.nasa.gov/data_and_products/formats/cpf.html

acts slightly off from the center of the main body. Furthermore, all these accelerations change with time and location, therefore the aforementioned Keplerian orbit is not applicable in those more realistic cases.

A Keplerian orbit can relatively easily be propagated forward (analytically) in time by changing the true anomaly θ based on the known orbital elements, since only that orbital element changes with time in this representation. However, for realistic perturbed orbits the propagation becomes more complex. One has to set up a dynamic orbit propagator that, for example, uses integrators like Runge-Kutta-Fehlberg or Dormand-Prince to solve non-linear equations such as those presented in Equation (4.3) (Montenbruck et al., 2002). This means that at every point in time the accelerations acting on the satellite have to be calculated given the state vector; for the air drag for example, one needs the altitude (a function of the satellite's position) to get the atmospheric density, the satellite's velocity magnitude and direction (from the state vector), the drag coefficient of the satellite (usually a constant), and the frontal surface area (a function of the attitude of the spacecraft). So, if all the accelerations are known at a point in time one can use a time step to get the next position and velocity and repeat the process.

Depending on what integrator is chosen the errors in every step may add up and the solution may become less accurate over time. It is also important to understand that this is a numerical method, and thus one needs to go through all the previous time steps to end up at a desired time.

Analytical methods exist as well, which can propagate orbits with some basic perturbations added. One such example is the SGP4 propagator that propagates TLEs (Vallado et al., 2006). This propagator takes into account the lower order spherical harmonic gravity (J_2 and J_3), can deal with an empirical formulation of atmospheric drag, and takes into account 3rd body perturbations from the Sun and Moon. It is more accurate than a Keplerian orbit propagation and for sure has many uses, but will never have centimeter level accuracy and for low Earth orbits (LEO) quickly starts deviating up to multiple kilometers from the real orbit (Vallado et al., 2006).

4.2.2 Precise orbit determination

Before one can propagate an orbit, one needs an orbit. A way to get an orbit is create a theoretical one or to determine an orbit based on observations. Whilst different kinds of orbit determination exist, the focus for now is on precise orbit determination. Precise orbit determination (POD) is the procedure of determining orbits of satellites at the centimeter or sub-centimeter level. See for an extensive review of the procedure e.g. Selvan et al. (2023), though, they do not mention VLBI as part of their work. Precise orbit determination is usually employed as a post-processing procedure to allow for the gathering of all necessary data.

Precise orbit determinations is particularly of interest for satellites that perform measurements which are at the centimeter level; if such measurements are done, but the orbit is only known at the meter level precise, the measurements are limited by this and can only be considered to be at the meter level precise

as well. For monitoring sea level rise at the millimeter level, precise positioning using GNSS satellites, and missions like Genesis in which millimeter frame ties are tried to be achieved (Delva et al., 2023), precise orbit determination is a necessity.

In order to determine a satellite orbit on centimeter level many gravitational and non-gravitational perturbations have to be taken into account next to the zero order gravitational attraction of the main body, as was described in Section 4.2.1. In order to achieve a precise orbit, this also means that the shape, orientation, and center of mass of the satellite should be known with a certain precision (Selvan et al., 2023).

There are different observations that can be used to determine orbits, or similarly locations (through which also an orbit can be fitted), such as ranges, Doppler measurements, or angle measurements (Selvan et al., 2023).

Different methods for POD exist, such as kinematic, reduced dynamic, and full dynamic, but in all cases it involves observations of the satellite or object (Selvan et al., 2023).

In kinematic orbit determination, no force models are used to estimate the orbit; each orbit position determined is independent of the others. In this method, one obtains a position and velocity at each of the observations. On the plus side, no force models are assumed, but on the down side, orbit prediction outside of the found orbit points is hardly possible due to the lack of knowledge on what influences the predicted orbit points.

In reduced dynamic orbit determination, only simplified force models are used to integrate the equations of motion of the satellite, and empirical accelerations are added to account for the unmodeled forces.

In full dynamic orbit determination, as many force models as possible are used to integrate the equations of motion of the satellite, while minimizing the residuals of the observations. This means the orbit is fully described by the used models, fitted best to the observations. The consequence is that the achieved solution is very sensitive to the accuracy of the used models. These orbit solutions are well suited for orbit prediction, if the same models are used as during the orbit determination.

Although dynamic and kinematic POD have their specific use cases, in most cases reduced dynamic POD is used (Selvan et al., 2023). In any dynamic case a (full or reduced) force model, like for example in Equation (4.3), is used to set up the the equations of motion which can be integrated using a numerical integrator. Using a least-squares estimator or Kalman filter the observations are used to reduce the O-C, like is done in VLBI analysis, and therefore finding the best orbit description given the observations.

4.2.3 Satellite observations with VLBI

Satellite observations for the sole purpose of orbit determination has been done since a long time ago. Deep space missions such as Voyager 1 and Voyager 2 (Campbell et al., 1983), Cassini-Huygens (Antreasian et al., 2008), Hayabusa 2 (Takeuchi et al., 2022), and Gaia (Fiori et al., 2022) have made use of satellite observations to determine their orbits for various reasons, albeit not

always using VLBI. Upcoming missions such as ESA's Jupiter Icy Moons Explorer (JUICE) will use VLBI for orbit determination through a system called Planetary Radio Interferometry and Doppler Experiment (PRIDE) (Duev et al., 2016), which will determine the lateral position and the radial velocity of the spacecraft. In such cases VLBI plays primarily a role in lateral position determination.

The observation of artificial radio sources such as satellites and lunar rovers using VLBI has not been done much within the geodetic VLBI community and the IVS. Only a handful of experiments in the past have attempted this and were successful (Klopotek et al., 2019; Tornatore et al., 2014). It should be noted that some of those experiments, and other space missions, have used a method, or signals from it, called Delta Differential One-way Ranging (Delta-DOR) (Fiori et al., 2022; Klopotek et al., 2019). Delta-DOR is slightly different from the method normally used in geodetic VLBI, and especially VGOS, since it alternates between observing only the source of interest and a nearby quasar, instead of using broadband synthesis (Petrachenko et al., 2012b). Recently though, the AuScope project in Australia has conducted multiple experiments using VGOS telescopes to observe GNSS satellites at GNSS frequencies (Schunck et al., 2026, March). They were able to estimate station positions to the meter level using rather narrow-band GNSS signals. Experiments like this, although not using the typical VGOS frequencies and thus having reduced performance, are key in understanding how VGOS can technically observe satellites.

In simulation studies the observing satellites has been envisioned and investigated plentifully. Observations of GNSS satellites, if equipped with a VLBI transmitter in the future, could aid in the direct transfer of the VLBI determined Earth rotation parameter UT1-UTC to the GNSS derived reference frame (Böhm and Wolf, 2025; Plank et al., 2017; Sert et al., 2022). Observations of other geodetic satellites, like the LAser GEOdynamics Satellite (LAGEOS)[4], have also been investigated with the aim of POD and geodetic parameter estimation, though they are passive satellites and will never emit a signal that can be detected by VLBI (Klopotek et al., 2020).

In recent times the focus within the geodetic VLBI community is more on ESA's Genesis mission, which is discussed in detail the next Section.

4.2.4 The Genesis mission

Genesis is an upcoming mission from ESA, the European Space Agency, that aims to create space ties between the four main space geodetic techniques (Delva et al., 2023). The mission will feature a 400 kg satellite in a near polar orbit at an inclination of 95 ° and at an altitude of 6000 km. The instruments onboard the satellite allow it to be observed by all four main space geodetic techniques. Therefore, it will feature a laser retro reflector for SLR, a GNSS receiver, a DORIS receiver, and a VLBI signal transmitter in the form of three antennas.

[4]LAGEOS-1, -2 at the ILRS website, https://ilrs.gsfc.nasa.gov/missions/satellite_missions/current_missions/lag1_general.html#info

The goal of Genesis brings with it many difficulties, specifically for the orbit and instruments. The chosen orbit altitude is similar to the SLR satellite LAGEOS, but is a compromise for the other techniques (Chatzinikos et al., 2026). For VLBI the orbit should be as high as possible to allow it being observed by as large baselines as possible, for DORIS it should not be too high to avoid that too many DORIS beacons can be received at the same time causing Doppler congestion, and for GNSS a lower orbit is slightly preferred to make sure that as many GNSS satellites as possible are visible to the GNSS receiver. Instrument wise, it is assumed that SLR and GNSS are not impacted in such a way that causes major difficulties for proper working onboard of the Genesis satellite. However, the two techniques that have significant changes with respect to their normal operation are DORIS and VLBI (VGOS in the case of Genesis). For DORIS a method needs to be implemented that allows the receiver to distinguish the many signals it will receive due to its higher altitude of 6000 km than normally used 1400 km or lower (Auriol and Tourain, 2010). Solutions have been found to alleviate the Doppler congestion problem at least to some extend by shifting the beacon frequencies (Moyard et al., 2023, November). For VGOS a broadband and polarized transmitter is needed to be comparable to nominal quasar observations. Together, these two requirements have significant impact on the design of the VLBI transmitter and leads (as of writing) to a design of 3 different separate antennas. This means that, firstly, 3 radio emission points are measured and need to be combined into one group delay to work with current VLBI analysis programs. Secondly, phase center variations and phase center offsets are expected in the 3 antenna design, as is commonly taken care of in the case of GNSS, but is not known for VLBI. Both these challenges mean that observing Genesis will be very different from observing one single radio source like a quasar and needs a lot of technical investigations.

Since Genesis has not yet been launched, many simulation studies have been carried out to assess different aspects and challenges related to the observation of Genesis using VGOS, of which the majority are focused on VLBI analyses and the higher level impact (on reference frames, EOPs, and orbits) of Genesis. For example, simulations have looked at the optimization of observation cadences between quasars and satellites (Schunck et al., 2024), the effect of different orbit types on Genesis derived ITRFs (Wolf et al., 2025), as well as investigations between ITRFs, and their ties, derived from quasar observations, satellite observations, and from both (Kern et al., 2026; Schunck et al., 2024). Most of these studies show that frame ties on millimeter level should be possible. The study by Schunck et al. (2024) showed that observation cadence of at minimal 5 minutes for Genesis in a quasar and Genesis observed session would impact the geodetic parameters and station positions minimally. The study as presented in Section 5.2.1 shows that the chosen orbit has a minimal effect on the overall performance and that a POD accuracy of a few cm should be obtainable.

As mentioned in Section 3.5, simulation studies tend to be too optimistic or at least very dependent on their input parameters. A study, as presented in Section 5.2.2, combined real data and simulated data based on real data ("hybrid" data), with the aim of achieving more realistic absolute assessments

of the impact of Genesis observations in VGOS sessions. Though some more investigation is needed, the study showed that based on only real data, indeed a 5 minute cadence for satellite observations in VGOS sessions would lead to minimal degradations of estimated EOPs. Furthermore, by combining real data and simulated data based on real data, the POD showed much degraded results in the accuracy, which was at decimeter level instead of at the other, pure simulation based, studies' few centimeter level. Also, the station position repeatability became unexpectedly large at lower mean repeat time for Genesis observations, while the EOP were not significantly more impacted. This study highlights the need to understand real world induced errors, which are currently unaccounted for in simulations and might lead to over optimistic assessments and expectations.

Also, purely real experiments have been done in the preparation of Genesis, next to the aforementioned simulation and hybrid studies. These include observation campaigns by AuScope (as mentioned in Section 4.2.3), which tested the whole chain from the observation of GNSS satellites until analysis using VGOS telescopes, albeit at non-VGOS frequencies. Their main results are that SP3 orbit files should be used in the correlation and fringe fitting process, that the differences between the near field delay models of Klioner (Klioner, 1991) and Duev (Duev et al., 2012) were on few ps level, tracking in steps larger than 10 seconds lead to significant errors and thus constant tracking is suggested, and frame ties between Galileo and VGOS were achieved on the decimeter level if NNT constraints were applied. Another real ongoing experiment is done using normal 24-hour VGOS sessions using the proposed Genesis frequency setup, which is different from the optimal quasar observation frequencies due to the limitations in what frequencies Genesis is allowed to transmit the VLBI signals. Their results have shown that the use of this frequency setup shows no problems so far.

Despite the presented research, many challenges remain to be investigated; (1) the determination of phase center variations and phase center offsets as a function of observation nadir angle, azimuth, and possibly temperature, taking into account the 3 distinct antennas, (2) the technical hurdles for telescopes to be able to track moving satellites, (3) the correlation and fringe fitting in case a signal comes from 3 distinct sources (antennas) that need to be combined into one single group delay, and (4) the cadence of both quasars and Genesis observations within a session and the cadence of sessions observing Genesis.

Chapter 5

Summary of research and future work

In this chapter summaries are given of the appended paper and the not appended research works, as well as a discussion on the planned future work.

5.1 Summary of appended papers

5.1.1 Source structure informed scheduling for VGOS intensive sessions

The performance of VGOS is not yet at the level that is required to fulfill the millimeter level GGOS requirements. This is among others due to the mismodeling of error sources and (geo)physical phenomena. One of the error sources that limits VGOS to the reach the GGOS millimeter requirements is radio source structure. Radio source structure is observable in quasars in the form of jet-like structures, while the quasars are usually assumed to be compact radio sources for geodetic purposes. The radio source structure manifests itself in the form of motion of the radio source emission and variations in flux density between the core and jet components which can shift the observed radio source position. Such shifts affect the geodetic analysis when the source positions are assumed to be fixed during the analysis.

While research has been done on mitigating these effects in different parts of the geodetic VLBI experiments, such as during the correlation and analysis steps (Jaron et al., 2025; Kareinen et al., 2024), the method of trying to avoid source structure all together by scheduling observations only in favorable conditions has not yet been done. Ideally, observations could only be scheduled if the angle between the jet direction and the projected baseline onto the source plane, called the α-angle, is close to 90 degrees. In such cases the radio source structure, in the form of the movement of the radio emission center, which is in most cases along the jet direction, should have a minimal effect on the measured time delay (Plank et al., 2016).

In order to test this hypothesis, a scheduling constraint has been applied to

the VGOS intensive session series VGOS-INT-C which only allows observations of quasars when the α-angle is larger than 45 degrees. The results from these sessions can be compared to the results from the unconstrained VGOS-INT-B sessions, which are observed on the same baseline between Onsala, Sweden, and Ishioka, Japan, in close temporal vicinity.

The comparison of the VLBI analyses of the unconstrained VGOS-INT-B and α-angle constrained VGOS-INT-C showed that the constraint did not improve the session performance nor the estimation of UT1-UTC. Nevertheless, it can be shown that the constraint avoids radio source structure to some extend. This is demonstrated by the lower root mean square (RMS) of the post-fit residuals for VGOS-INT-C compared to VGOS-INT-B across source groups with increasing source structure. This indicates that even when VGOS-INT-C observed quasars with generally more source structure, this source structure was not observed as much due to the favorable, source structure avoiding, observation conditions. Furthermore, at least a 5 % lower unweighted RMS of all post-fit residuals is found in VGOS-INT-C compared to VGOS-INT-B. These findings were further strengthened by only analyzing observations made at elevations above 15°, which on its own indicates that the troposphere estimation has a bigger impact than source structure at low elevations.

Overall, for both series, the RMS of post-fit residuals decreases with increasing α-angle, which is a very strong indication that source structure is most observed when the α-angle is close to 0°. An unexpected results was that for both sessions the mean signal-to-noise ratio (SNR) increases with increasing α-angle. This finding could be used to further optimize SNR based scheduling. Both found trends were steeper in VGOS-INT-B than in VGOS-INT-C.

To conclude, the study shows strong indications that radio source structure can partially be avoided by using an α-angle scheduling constraint. However, in case of the intensive sessions analyzed, it did not have a significant impact on the session performance or estimation of the UT1-UTC parameter. Finally, it should be noted that the applied scheduling constraint is unsuitable for various sources because the jet angle describes their source structure inadequately, mainly because the ratio emission movement does not align well with the jet angle direction.

5.2 Summary of not appended work

5.2.1 Simulating and analysing VGOS observations for Genesis orbits and EOP determination

Authors: R. Wolfs and R. Haas.

Research presented as a poster at the European Geoscience Union (EGU) in April 2025. Version 2 update uploaded to Chalmers website March 2026. No publication planned.

Motivation

The Genesis mission of ESA will allow for satellite observations using VGOS. From previous work POD of Genesis should be possible (Klopotek et al., 2020). At the time of conducting the study it was not yet decided if the satellite would by put in a 60° or 95° inclined orbit. Therefore, a comparison of the POD performance of Genesis for the two inclinations was done, using VGOS observations. This analysis was extended to also assess the POD performance of orbit injection errors. This aim is to find out if one of the two inclinations is highly preferred and if orbit injection errors are of critical influence.

Method

The C5++ VLBI analysis software (Hobiger et al., 2010) is able to simulate and analyze both quasar and satellite VLBI observations (Klopotek et al., 2020). A primarily investigation is done, through 24 hour session simulations, to investigate the POD performance for a Genesis like orbit. Five orbits at 60 degrees inclination are investigated, at different eccentricities and altitudes similar to (exaggerated) orbit injection errors that could occur, denoted as orbits SA to SE (see Figure 5.1). Next to that also one orbit at 95 degrees inclination, denoted as SF, is investigated.

Simulations were done to generate NGS databases using Vex files generated by *Viesched++* for a VGOS network of 14 stations, two-line element (TLE) orbit files, and a standard simulation setup. Since the simulations are run for just 1 day, on March 21st 2025, the network geometry aspect is partially evened out by using the satellite orbit at 8 different RAANs. Each simulation is conducted 30 times in Monte Carlo fashion to get a more realistic assessment using 3 simulated error sources (clock, troposphere, and measurement errors, see Section 3.5). Genesis was observed every 5th minute (Schunck et al., 2024), whilst quasars were observed roughly every 30 seconds. The observation integration time for Genesis was set to 10 seconds.

In the analysis of the simulated NGS databases the orbit, ERPs (i.e. no nutation), and station positions are estimated. The initial orbit in the analysis is the original orbit used for the simulation of the observations, but perturbed randomly in each direction using a sigma of 30 meters. To assess the POD performance the unperturbed orbit points are compared to the estimated orbit points at 5 minute intervals in each of the runs. The ERP estimation is assessed by checking the differences between the input apriori values and the estimated ones. The station positions are evaluated by calculating the station repeatabilities, as well as the corresponding amount of satellite and quasar scans.

Results and discussion

The results show that the 95° inclined orbit performed slightly worse than a 60° inclined orbit in terms of POD by at most 20 %, which is equal to about 0.25 mm (see Figure 5.1). For the 60° inclined orbit both the changes in the assessed altitudes and eccentricities show no large impact.

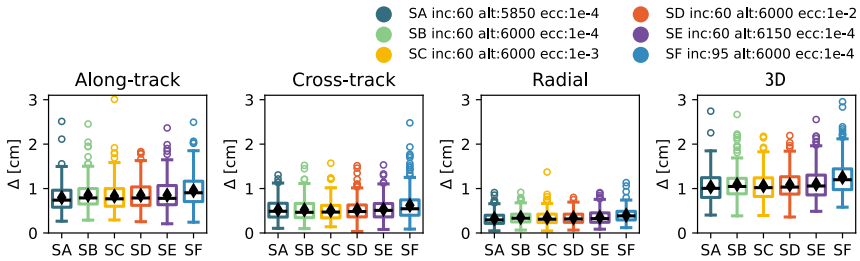

Figure 5.1. Box plots of RMS of all orbit solutions (8 RAANs and 30 Monte Carlo runs) w.r.t. input orbit per orbit type. Black diamonds: mean, black horizontal line: median.

The actual RAAN of the orbit does have an impact on the POD performance of about 25% (see Figure 5.2). This is likely related to the network geometry and the RAAN, which is one of the orbital elements that especially affects the observation geometry and occurrences. It is also clear that in parts of the satellite orbit where the satellite can be observed less, such as above South-America and Antarctica, the POD performance is most affected (see Figure 5.3).

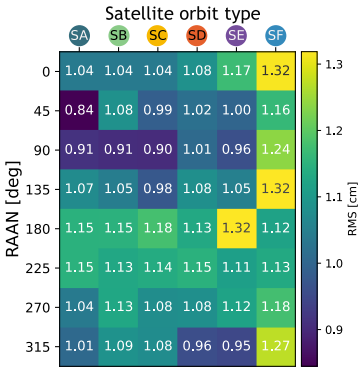

Figure 5.2. 24 hour orbit arc 3D RMS for satellite orbit type versus RAAN.

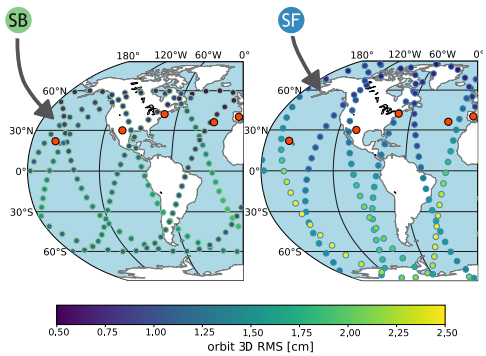

Figure 5.3. Epoch wise 3D orbit RMS for orbit type at 0 deg RAAN, for 2 orbit types.

Some further results were found of which no figures or tables are included. The station repeatabilities some slight changes could be observed between the orbit types, which were at most 0.5 cm in the up component. Also stations that are relatively isolated in a network, such as KOKEE12M, benefit from having less satellite scans, since those satellite observations are done at relatively low elevations, which is disadvantageous.

In terms of ERP estimation there were no large differences observed.

The work done shows that the orbit injection errors have some, but no significant impact on the POD performance. The chosen orbit inclination does

have a significant impact, which means that the 60° inclined orbit performs slightly better than the 95° one. While station position repeatabilities are slightly affected, and ERP are almost not not.

5.2.2 A hybrid approach using real and simulated data to assess the performance of VGOS sessions with added Genesis observations

Authors: R. Wolfs and R. Haas.
Research presented as a poster at the European Geoscience Union (EGU) in May 2026. Further research and manuscript submission planned for 2026.

Motivation

The Genesis mission of ESA will be observed by VGOS. What is so far still unclear is how often the satellite should be observed in between quasar observations. Observing the satellite means that less quasars can be observed and consequently the geodetic parameter estimation might be impacted. Some simulation work has investigated this, but has not focused on the impact on EOP estimation, did not estimate the orbit, and was purely based on simulated data (Schunck et al., 2024).

In this work a method using hybrid data, meaning both real data and simulated data based on real data, is used to assess the observation cadence of Genesis and the impact on the estimation of station positions, EOPs, and the satellite orbit. The aim is to get a more realistic assessment since real data is incorporated in the analysis.

Method

The study consists of two parts: First an assessment is made on the removal of scans from real VGOS 24 hour sessions, as if Genesis is being observed at that time, and second, the removed scans are substituted with simulated satellite observations using results from real sessions to simulate the error source contributions (clock, troposphere, and measurement noise). The removal or substitution of quasar scans is based on the visibility of Genesis, using the latest published Genesis orbit by ESA.

For the first part the focus is on a minimum repeat time (MRT) of Genesis observations between 1 and 15 minutes. This has been done before in simulation studies, but so far not using real data. In our study we analyze how the removal of quasar scans impacts the estimation of the EOPs and station position repeatabilities. This gives insight in the practical aspects of scheduling VGOS sessions that include Genesis observations (which are not used in the analysis).

The second part builds upon the first part by, instead of removing the quasar observations, substituting the removed quasar observations with simulated Genesis observations. Still, the main focus here is on the MRT as the main variable. However, with the use of real and reality based simulated data, we

aim to create a more realistic assessment of the impact of Genesis observations on the estimation of EOPs, station positions, and the satellite orbit.

Results and discussion

The results of the first part show that the station repeatabilities (Figure 5.4) and EOPs (Figure 5.5) are affected most significantly when MRTs are used below 5 minutes.

This suggest that the estimation of EOPs and station positions is impacted by including Genesis observations with a MRT of at most 5 minutes. This means that maybe special VGOS sessions need to be considered to supply the space ties between the Genesis and VLBI reference frames and keep the estimation of operation product EOPs and station positions for separate dedicated sessions.

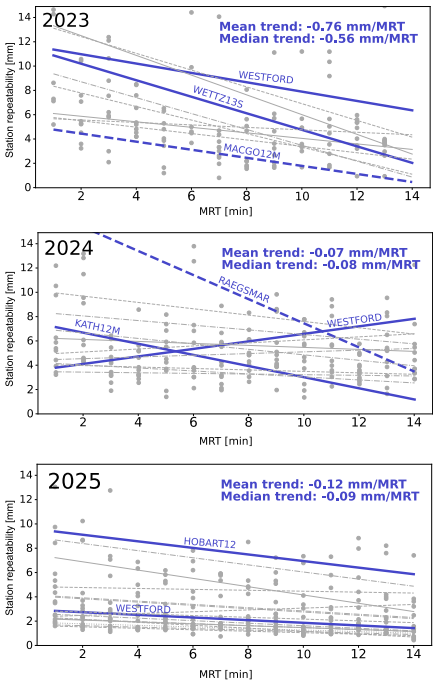

Figure 5.4. Station repeatabilities and trendlines per MRT, with interesting trendlines highlighted.

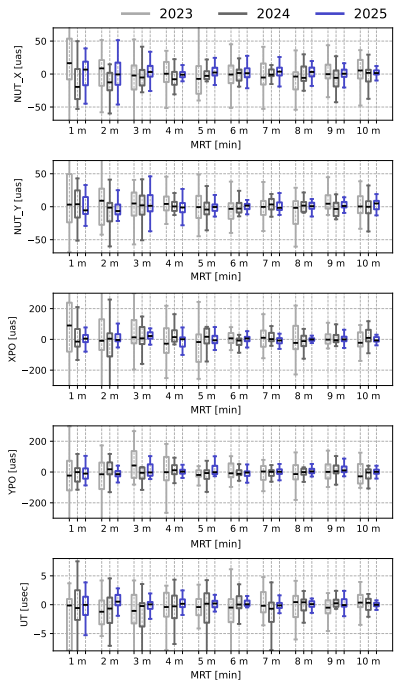

Figure 5.5. Boxplots of EOP offsets from the means of MRTs of 10-15 min, per MRT.

The results of the second part, where the removed real quasar observations were substituted with simulated Genesis observations, show that the station repeatabilities and EOPs are affected similarly like in the part where quasar observations were only removed. However, the magnitude of especially the station repeatabilities was degraded a lot (not shown in the thesis), especially at lower MRTs.

The orbit estimation showed wildly varying performance between sessions (see Figure 5.6), which most strikingly is considerably worse than previous

work. The reason for the generally worse orbit estimation might be due to the observations of Genesis being clustered in certain parts of the orbit (see Figure 5.7). Such clustering means that there are no observations in certain parts of the orbit, given that Genesis has a orbital period of about 4 hours, which is clearly visible in the period of the orbit errors. That consequently means that the orbit estimation performance will be degraded since that part of the orbit is unconstrained by observations. This degraded estimated orbit then influences the estimation of the EOP and the station positions and can be the reason for the degradation observed in those parameters for this case.

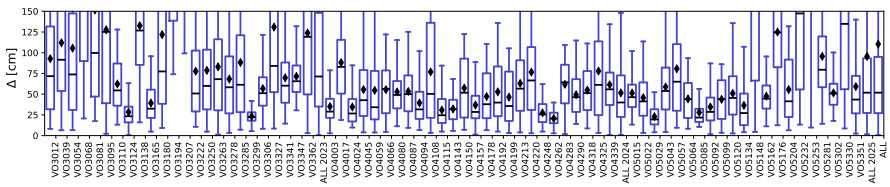

Figure 5.6. Boxplots of 3D differences between input and estimated orbit per session at an MRT of 5 min.

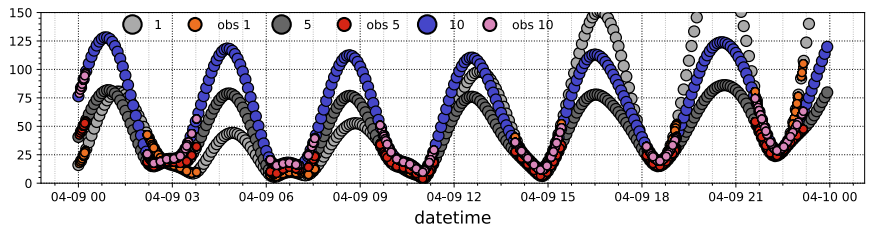

Figure 5.7. The 3D differences between input and estimated orbit for VO5099 together with indicators for when the satellite was observed, for 3 different MRTs.

More work needs to be done to finetune the simulated satellite observations using outputs from real session analysis, as well as on investigating the effect of the station network on the orbit estimation performance.

5.3 Future work

The two main topics that guide this thesis on radio source structure mitigation and incorporating satellite observations in VGOS sessions, allow for plenty of possible follow up studies.

Radio source structure The research on radio source structure mitigation suggest at least two worthwhile follow-up possibilities.

Firstly, there was a strong indication that that radio source structure was mitigated by applying the scheduling constraint to VGOS-INT-C, however, no significant performance improvement was observed session wise and in the

estimation of the UT1-UTC. The reason for this could be that, even though the data set spanned three years, the session to session changes and errors have a larger magnitude than the source structure. An idea would be to set up a dedicated experiment that conducts a 24 hour pseudo intensive session, that every hour alternate between applying and not applying the scheduling constraint.

Secondly, the exclusion of observations below 15° elevation made the source structure contributions more visible. This warrants a further investigation into the low elevation observation errors, which seem to dominate the overall performance of the session. There are indications that the ionosphere causes issues and it is well known that the troposphere estimation is worse at lower elevations as well, especially for intensive sessions. Since these relatively high residual low elevation observations in the cusp of the mutual sky are important in the determination of UT1-UTC, it would be advantageous to investigate these issues.

Satellite observations The studies done on satellite observations with VGOS have shown some insights w.r.t the removal of quasar observations in real sessions and the validity, and potentially overly optimistic outcomes, of satellite observation simulations. Therefore, there are at least 2 possible future investigations to be considered.

First of all, the work in Section 5.2.2 is planned to be further extended with the aim of publishing it in a peer reviewed journal. As mentioned in that section, the main things to be done are the finetuning of the simulated satellite observations which are based on real session results, as well as investigating the effect of the station network on the performance of the satellite orbit estimation. It would be very worthwhile to find some key points that can help in optimizing future scheduling of Genesis observations and finding a more realistic estimate of the performance of precise orbit determination using VGOS observations.

Secondly, the investigation of removing quasar observations from real VGOS-OPS sessions has applications beyond the scheduling of satellite observations in VGOS-OPS sessions. VGOS-OPS sessions have a considerable turn around time, and investigations are ongoing into reducing this. One proposed solution is to reduce the amount of quasar observations done by about a factor of 2, however our analysis shows that the removal of as low as 10% of quasar observations already leads to a slight degradation of the estimated EOPs and station repeatabilities. It would be good to investigate this a bit further, and possibly include this as well in the planned peer reviewed paper.

Bibliography

Altamimi, Z., Rebischung, P., Collilieux, X., Métivier, L., & Chanard, K. (2023). ITRF2020: An augmented reference frame refining the modeling of nonlinear station motions. *Journal of Geodesy*, *97*(5), 47.

Anderson, J. M., & Xu, M. H. (2018). Source Structure and Measurement Noise Are as Important as All Other Residual Sources in Geodetic VLBI Combined. *Journal of Geophysical Research: Solid Earth*, *123*(11).

Angermann, D., Pail, R., Seitz, F., & Hugentobler, U. (2022). *Mission earth: Geodynamics and climate change observed through satellite geodesy.*

Antreasian, P., Ardalan, S., Criddle, K., Ionasescu, R., Jacobson, R., Jones, J., MacKenzie, R., Parcher, D., Pelletier, F., Roth, D., Thompson, P., & Vaughan, A. (2008). Orbit determination processes for the navigation of the Cassini-Huygens mission. In *Spaceops 2008 conference*. American Institute of Aeronautics; Astronautics.

Ashby, N. (2003). Relativity in the global positioning system. *Living Reviews in Relativity*, *6*(1), 1.

Auriol, A., & Tourain, C. (2010). DORIS system: The new age. *Advances in Space Research*, *46*(12), 1484–1496.

Bar-Sever, Y., Haines, B., Bertiger, W., Desai, S., & Wu, S. (2009). Geodetic Reference Antenna in Space (GRASP) – a Mission to Enhance Space-based Geodesy.

Biancale, R., Pollet, A., Coulot, D., & Mandea, M. (2017). E-GRASP/Eratosthenes: A mission proposal for millimetric TRF realization.

Blandford, R., Meier, D., & Readhead, A. (2019). Relativistic jets from active galactic nuclei. *Annual Review of Astronomy and Astrophysics*, *57*, 467–509.

Boehm, J., Niell, A., Tregoning, P., & Schuh, H. (2006). Global mapping function (GMF): A new empirical mapping function based on numerical weather model data. *Geophysical Research Letters*, *33*(7).

Böhm, J., Böhm, S., Boisits, J., Girdiuk, A., Gruber, J., Hellerschmied, A., Krásná, H., Landskron, D., Madzak, M., Mayer, D., McCallum, J., McCallum, L., Schartner, M., & Teke, K. (2018). Vienna VLBI and Satellite Software (VieVS) for Geodesy and Astrometry. *Publications of the Astronomical Society of the Pacific*, *130*(986), 044503.

Böhm, J., & Wolf, H. (2025). Opportunities with VLBI transmitters on satellites. In J. T. Freymueller & L. Sánchez (Eds.), *Together again for geodesy* (pp. 3–8). Springer Nature Switzerland.

Campbell, J., Synnott, S., & Bierman, G. (1983). Voyager orbit determination at Jupiter. *IEEE Transactions on Automatic Control*, *28*(3), 256–268.

Charlot, P. (1990). Radio-source structure in astrometric and geodetic very long baseline interferometry. *The Astronomical Journal*, *99*, 1309.

Charlot, P., Jacobs, C. S., Gordon, D., Lambert, S., Witt, A. d., Böhm, J., Fey, A. L., Heinkelmann, R., Skurikhina, E., Titov, O., Arias, E. F., Bolotin, S., Bourda, G., Ma, C., Malkin, Z., Nothnagel, A., Mayer, D., MacMillan, D. S., Nilsson, T., & Gaume, R. (2020). The third realization of the International Celestial Reference Frame by very long baseline interferometry. *Astronomy & Astrophysics*, *644*, A159.

Chatzinikos, M., Delva, P., Chang, M., Aghouraf, W., Coulot, D., & Pollet, A. (2026). An ensemble MCDM strategy for orbit design in Genesis-like missions. *Advances in Space Research*, *77*(2), 1381–1403.

Delva, P., Altamimi, Z., Blazquez, A., Blossfeld, M., Böhm, J., Bonnefond, P., Boy, J.-P., Bruinsma, S., Bury, G., Chatzinikos, M., Couhert, A., Courde, C., Dach, R., Dehant, V., Dell'Agnello, S., Elgered, G., Enderle, W., Exertier, P., Glaser, S., … Zajdel, R. (2023). GENESIS: Co-location of geodetic techniques in space. *Earth, Planets and Space*, *75*(1), 5.

Desai, S. D. (2002). Observing the pole tide with satellite altimetry. *Journal of Geophysical Research: Oceans*, *107*(C11), 7-1-7–13.

Duev, D. A., Pogrebenko, S. V., Cimò, G., Molera Calvés, G., Bocanegra Bahamón, T. M., Gurvits, L. I., Kettenis, M. M., Kania, J., Tudose, V., Rosenblatt, P., Marty, J.-C., Lainey, V., De Vicente, P., Quick, J., Nickola, M., Neidhardt, A., Kronschnabl, G., Ploetz, C., Haas, R., … Witasse, O. (2016). Planetary Radio Interferometry and Doppler Experiment (PRIDE) technique: A test case of the Mars Express Phobos fly-by. *Astronomy & Astrophysics*, *593*, A34.

Duev, D. A., Calves, G. M., Pogrebenko, S. V., Gurvits, L. I., Cimo, G., & Bahamon, T. B. (2012). Spacecraft VLBI and Doppler tracking: Algorithms and implementation. *Astronomy & Astrophysics*, *541*, A43.

Fey, A. L., & Charlot, P. (1997). VLBA observations of radio reference frame sources. II. astrometric suitability based on observed structure. *The Astrophysical Journal Supplement Series*, *111*(1), 95.

Fiori, F., Tortora, P., Zannoni, M., Ardito, A., Menapace, M., Bellei, G., Budnik, F., Morley, T., Mercolino, M., & Orosei, R. (2022). Deep space orbit determination via Delta-DOR using VLBI antennas. *CEAS Space Journal*, *14*(2), 421–430.

García-Carreño, P., González-García, J., Patino-Esteban, M., Beltrán-Martínez, F. J., Bautista-Durán, M., López-Espí, P. L., & López-Pérez, J. A. (2022). New Cable Delay Measurement System for VGOS Stations. *Sensors*, *22*(6), 2308.

Gattano, C., & Charlot, P. (2021). Characterizing the astrometric instability of extragalactic radio source positions measured with geodetic VLBI. *Astronomy & Astrophysics*, *648*, A125.

Gipson, J., & Baver, K. (2015). Minimization of the UT1 Formal Error Through a Minimization Algorithm.

Gipson, J. (2010, December). An introduction to Sked. In D. Behrend & K. D. Baver (Eds.), *IVS 2010 general meeting proceedings, international VLBI service for geodesy and astrometry* (pp. 77–84).

Gipson, J., & Baver, K. (2016). Improvement of the IVS-INT01 sessions by source selection: Development and evaluation of the maximal source strategy. *Journal of Geodesy*, *90*(3), 287–303.

Gross, R. S., & Vondrák, J. (1999). Astrometric and space-geodetic observations of polar wander. *Geophysical Research Letters*, *26*(14), 2085–2088.

Haas, R., Scherneck, H.-G., & Schuh, H. (1997). Atmospheric loading corrections in geodetic VLBI and determination of atmospheric loading coefficients. *Proceedings of the 12th Working Meeting on European VLBI for Geodesy and Astrometry*.

Haas, R., Vaernius, E., Matsumoto, S., & Schartner, M. (2021). Observing UT1-UTC with VGOS.

Herring, T. A., Davis, J. L., & Shapiro, I. I. (1990). Geodesy by radio interferometry: The application of kalman filtering to the analysis of very long baseline interferometry data. *Journal of Geophysical Research: Solid Earth*, *95*(B8), 12561–12581.

Himwich, E. (2000). Introduction to the field system for non-users. *International VLBI Service for Geodesy and Astrometry: 2000 General Meeting Proceedings*.

Hobiger, T., Gotoh, T., Otsubo, T., Kubooka, T., Sekido, M., Takiguchi, H., & Takeuchi, H. (2010). C5++ - Multi-technique Analysis Software for Next Generation Geodetic Instruments.

IAG Office. (2025). *IAG Geodesist's Handbook 2024*. International Association of Geodesy (IAG).

Jaron, F., Baldreich, L., Böhm, J., Charlot, P., Collioud, A., Gruber, J., Krásná, H., Martí-Vidal, I., Nothnagel, A., & Pérez-Díez, V. (2025). Mitigating source structure in geodetic VLBI on the visibility level.

Jaron, F., & Nothnagel, A. (2019). Modeling the VLBI delay for earth satellites. *Journal of Geodesy*, *93*(7), 953–961.

Johnston, G., Riddell, A., & Hausler, G. (2017). The international GNSS service. In P. J. Teunissen & O. Montenbruck (Eds.), *Springer handbook of Global Navigation Satellite Systems* (pp. 967–982). Springer International Publishing.

Kareinen, N., Zubko, N., Savolainen, T., Xu, M. H., & Poutanen, M. (2024). Mitigating the effect of source structure in geodetic VLBI by reweighting observations using closure delays and baseline-to-jet orientation. *Journal of Geodesy*, *98*(5), 38.

Kern, L., Wolf, H., & Böhm, J. (2026). Assessing the frame ties between VLBI observations to quasars and genesis. *IAG International Symposium on Reference Frames for Applications in Geosciences (REFAG2026), 2–4 March 2026: Abstract Book*.

Klioner, S. (1991). General relativistic model of VLBI observables. *Proceedings of AGU Chapman Conference on Geodetic VLBI: Monitoring Global Change*.

Klopotek, G., Hobiger, T., & Haas, R. (2017). Implementation of VLBI Near-Field Delay Models in the c5++ Analysis Software.

Klopotek, G., Hobiger, T., & Haas, R. (2018). Geodetic VLBI with an artificial radio source on the moon: A simulation study. *Journal of Geodesy*, *92*(5), 457–469.

Klopotek, G., Hobiger, T., Haas, R., Jaron, F., La Porta, L., Nothnagel, A., Zhang, Z., Han, S., Neidhardt, A., & Plötz, C. (2019). Position determination of the Chang'e 3 lander with geodetic VLBI. *Earth, Planets and Space*, *71*(1), 23.

Klopotek, G., Hobiger, T., Haas, R., & Otsubo, T. (2020). Geodetic VLBI for precise orbit determination of Earth satellites: A simulation study. *Journal of Geodesy*, *94*(6), 56.

Kostrichkin, I. M., Plavin, A. V., Pushkarev, A. B., & Butuzova, M. S. (2025). Evolution of parsec-scale jet directions in active galaxies. *Monthly Notices of the Royal Astronomical Society*, *537*(2), 978–990.

Landskron, D., & Böhm, J. (2018). VMF3/GPT3: Refined discrete and empirical troposphere mapping functions. *Journal of Geodesy*, *92*(4), 349–360.

McCarthy, T., & McCallum, L. (2025). The impact of observation losses on IVS-R1/R4 VLBI sessions. *Journal of Geodesy*, *99*(11), 84.

Montenbruck, O., Gill, E., & Lutze, F. (2002). Satellite orbits: Models, methods, and applications. *Appl. Mech. Rev.*, *55*(2), B27–B28.

Montenbruck, O., Hackel, S., & Jäggi, A. (2018). Precise orbit determination of the Sentinel-3A altimetry satellite using ambiguity-fixed GPS carrier phase observations. *Journal of Geodesy*, *92*(7), 711–726.

Moran, J. (1998). Thirty Years of VLBI: Early Days, Successes, and Future. *International Astronomical Union Colloquium*, *164*, 1–10.

Moyard, J., Mercier, F., & Couhert, A. (2023, November). Progress in the phase 0: DORIS on board Galileo.

Nilsson, T., & Haas, R. (2010). Impact of atmospheric turbulence on geodetic very long baseline interferometry. *Journal of Geophysical Research: Solid Earth*, *115*(B3), 2009JB006579.

Nilsson, T. (2022). The Current and Future Performance of VGOS. *International VLBI Service for Geodesy and Astrometry 2022 General Meeting Proceeding*.

Nilsson, T., Mora-Diaz, J. A., Raposo-Pulido, V., Heinkelmann, R., Karbon, M., Liu, L., Lu, C., Xu, B. S. M., & Schuh, H. (2017). Antenna axis offsets and their impact on VLBI derived reference frames. In T. van Dam (Ed.), *REFAG 2014* (pp. 53–58). Springer International Publishing.

Nothnagel, A., Artz, T., Behrend, D., & Malkin, Z. (2017). International VLBI service for geodesy and astrometry. *Journal of Geodesy*, *91*(7), 711–721.

Nothnagel, A. (2009). Conventions on thermal expansion modelling of radio telescopes for geodetic and astrometric VLBI. *Journal of Geodesy*, *83*(8), 787–792.

Nothnagel, A. (2019). The correlation process in very long baseline interferometry. *GEM - International Journal on Geomathematics*, *10*(1), 18.

Pany, A., Böhm, J., MacMillan, D., Schuh, H., Nilsson, T., & Wresnik, J. (2011). Monte Carlo simulations of the impact of troposphere, clock and measurement errors on the repeatability of VLBI positions. *Journal of Geodesy*, *85*(1), 39–50.

Pearlman, M. R., Noll, C. E., Pavlis, E. C., Lemoine, F. G., Combrink, L., Degnan, J. J., Kirchner, G., & Schreiber, U. (2019). The ILRS: Approaching 20 years and planning for the future. *Journal of Geodesy*, *93*(11), 2161–2180.

Pelton, J. N., Madry, S., & Camacho-Lara, S. (2017). *Handbook of satellite applications* (Vol. 1). Springer New York.

Petit, G., & Luzum, B. (Eds.). (2010). *IERS conventions (2010)*. Verlag des Bundesamts für Kartographie und Geodäsie.

Petrachenko, W. T., Niell, A. E., Corey, B. E., Behrend, D., Schuh, H., & Wresnik, J. (2012a). VLBI2010: Next generation VLBI system for geodesy and astrometry. In S. Kenyon, M. C. Pacino & U. Marti (Eds.), *Geodesy for planet earth* (pp. 999–1005). Springer Berlin Heidelberg.

Petrachenko, W. T., Niell, A. E., Corey, B. E., Behrend, D., Schuh, H., & Wresnik, J. (2012b). VLBI2010: Next Generation VLBI System for Geodesy and Astrometry. In S. Kenyon, M. C. Pacino & U. Marti (Eds.), *Geodesy for Planet Earth* (pp. 999–1005). Springer Berlin Heidelberg.

Plag, H. .-., Rizos, C., Rothacher, M., & Neilan, R. (2010). The global geodetic observing system (GGOS): Detecting the fingerprints of global change in geodetic quantities. In E. Chuvieco, J. Li & X. Yang (Eds.), *Advances in earth observation of global change* (pp. 125–143). Springer Netherlands.

Plank, L., Shabala, S. S., McCallum, J. N., Krásná, H., Petrachenko, B., Rastorgueva-Foi, E., & Lovell, J. E. J. (2016). On the estimation of a celestial reference frame in the presence of source structure. *Monthly Notices of the Royal Astronomical Society*, *455*(1), 343–356.

Plank, L., Hellerschmied, A., McCallum, J., Böhm, J., & Lovell, J. (2017). VLBI observations of GNSS-satellites: From scheduling to analysis. *Journal of Geodesy*, *91*(7), 867–880.

Rizos, C., & Willis, P. (Eds.). (2014). *Earth on the Edge: Science for a Sustainable Planet: Proceedings of the IAG General Assembly, Melbourne, Australia, June 28 - July 2, 2011* (Vol. 139). Springer Berlin Heidelberg.

Ryan, J. W., Clark, T. A., Coates, R. J., Ma, C., Wildes, W. T., Gwinn, C. R., Herring, T. A., Shapiro, I. I., Corey, B. E., Counselman, C. C., Hinteregger, H. F., Rogers, A. E. E., Whitney, A. R., Knight, C. A., Vandenberg, N. R., Pigg, J. C., Schupler, B. R., & Rönnäng, B. O. (1986). Geodesy by radio interferometry: Determinations of baseline vector, earth rotation, and solid earth tide parameters with the mark I very long baseline radio interferometry system. *Journal of Geophysical Research: Solid Earth*, *91*(B2), 1935–1946.

Saastamoinen, J. (1972). Atmospheric correction for the troposphere and stratosphere in radio ranging satellites. In *The use of artificial satellites for geodesy* (pp. 247–251). American Geophysical Union (AGU).

Schartner, M. (2025). Deriving a global troposphere model for space geodetic simulations based on an ML ensemble featuring uncertainty quantification. *Journal of Geodesy*, *99*(9), 72.

Schartner, M., & Böhm, J. (2019). VieSched++: A New VLBI Scheduling Software for Geodesy and Astrometry. *Publications of the Astronomical Society of the Pacific*, *131*(1002), 084501.

Schartner, M., Kern, L., Nothnagel, A., Böhm, J., & Soja, B. (2021). Optimal VLBI baseline geometry for UT1-UTC Intensive observations. *Journal of Geodesy*, *95*(7), 75.

Scherneck, H.-G., Haas, R., & Laudati, A. (2000). Ocean loading tides for, in, and from VLBI. *IVS 2000 General Meeting Proceedings*, 257–262.

Schmidt, M. (1963). 3C 273 : A star-like object with large red-shift. *Nature*, *197*(4872), 1040–1040.

Schuh, H., & Behrend, D. (2012). VLBI: A fascinating technique for geodesy and astrometry. *Journal of Geodynamics*, *61*, 68–80.

Schunck, D., McCallum, L., McCallum, J., & McCarthy, T. (2026, March). Comprehensive VLBI observations of Galileo satellites with the AuScope array.

Schunck, D., McCallum, L., & Molera Calvés, G. (2024). On the Integration of VLBI Observations to GENESIS into Global VGOS Operations. *Remote Sensing*, *16*(17), 3234.

Seeber, G. (1993). Satellite geodesy: Foundations, methods, and applications. *Science*, *262*, 775.

Seitz, M., Bloßfeld, M., Glomsda, M., Angermann, D., Rudenko, S., Zeitlhöfler, J., & Seitz, F. (2026). DTRF2020: The ITRS 2020 realization of DGFI-TUM. *Journal of Geodesy*, *100*(2), 15.

Sekido, M., & Fukushima, T. (2006). A VLBI Delay Model for Radio Sources at a Finite Distance. *Journal of Geodesy*, *80*(3), 137–149.

Selvan, K., Siemuri, A., Prol, F. S., Välisuo, P., Bhuiyan, M. Z. H., & Kuusniemi, H. (2023). Precise orbit determination of LEO satellites: A systematic review. *GPS Solutions*, *27*(4), 178.

Sert, H., Hugentobler, U., Karatekin, O., & Dehant, V. (2022). Potential of UT1–UTC transfer to the galileo constellation using onboard VLBI transmitters. *Journal of Geodesy*, *96*(10), 83.

Shabala, S. S., McCallum, J. N., Plank, L., & Böhm, J. (2015). Simulating the effects of quasar structure on parameters from geodetic VLBI. *Journal of Geodesy*, *89*(9), 873–886.

Sovers, O. J. (1994). Vertical ocean loading amplitudes from VLBI measurements. *Geophysical Research Letters*, *21*(5), 357–360.

Sovers, O. J., Fanselow, J. L., & Jacobs, C. S. (1998). Astrometry and geodesy with radio interferometry: Experiments, models, results. *Reviews of Modern Physics*, *70*(4), 1393–1454.

Takeuchi, H., Taniguchi, S., Ichikawa, T., Bellerose, J., Tarzi, Z., Farnocchia, D., Yoshikawa, M., Saiki, T., & Tsuda, Y. (2022). Chapter 5 - orbit determination for hayabusa2. In M. Hirabayashi & Y. Tsuda (Eds.), *Hayabusa2 asteroid sample return mission* (pp. 73–94). Elsevier.

Tornatore, V., Haas, R., Casey, S., Duev, D., Pogrebenko, S., & Calvés, G. M. (2014). Direct VLBI observations of global navigation satellite system signals. In C. Rizos & P. Willis (Eds.), *Earth on the edge: Science for a sustainable planet* (pp. 247–252). Springer Berlin Heidelberg.

Vallado, D., Crawford, P., Hujsak, R., & Kelso, T. (2006). Revisiting spacetrack report 3. *Collection of Technical Papers - AIAA/AAS Astrodynamics Specialist Conference, 2006*, *3*.

Vallado, D. A. (2001). *Fundamentals of astrodynamics and applications* (Vol. 12). Springer Science & Business Media.

Wahr, J. M. (1981). Body tides on an elliptical, rotating, elastic and oceanless earth. *Geophysical Journal of the Royal Astronomical Society*, *64*(3), 677–703.

Wakker, K. F. (2015). Fundamentals of astrodynamics. *TU Delft Repository, Delft*, 604–612.

Wang, J., Ge, M., Glaser, S., Balidakis, K., Heinkelmann, R., & Schuh, H. (2022). Impact of Tropospheric Ties on UT1-UTC in GNSS and VLBI Integrated Solution of Intensive Sessions. *Journal of Geophysical Research: Solid Earth*, *127*(11), e2022JB025228.

Wertz, J. R. (2001). *Mission geometry: orbit and constellation design and management: spacecraft orbit and attitude systems*. Microcosm Inc.

Wertz, J. R., Larson, W. J., Kirkpatrick, D., & Klungle, D. (1999). *Space mission analysis and design*. Microcosm ; Kluwer.

Whitney, A., Lonsdale, C., Himwich, E., Vandenberg, N., van Langevelde, H., Mujunen, A., & Walker, C. (2002). VEX file definition/example.

Whitney, A. R. (1974). *Precision geodesy and astrometry via very-long-baseline interferometry* [Doctoral dissertation, Massachusetts Institute of Technology].

Willis, P., Lemoine, F. G., Moreaux, G., Soudarin, L., Ferrage, P., Ries, J., Otten, M., Saunier, J., Noll, C., Biancale, R., & Luzum, B. (2016). The international DORIS service (IDS): Recent developments in preparation for ITRF2013. In C. Rizos & P. Willis (Eds.), *IAG 150 years* (pp. 631–640). Springer International Publishing.

Wolf, H., Kern, L. M., Steinmetz, S., & Böhm, J. (2025). Impact of the inclination of genesis on the VLBI terrestrial reference frame. *Book of Abstracts: European VLBI Group for Geodesy and Astronomy (EVGA)*, 65–65.

Xu, M. H., Anderson, J. M., Heinkelmann, R., Lunz, S., Schuh, H., & Wang, G. (2021a). Observable quality assessment of broadband very long baseline interferometry system. *Journal of Geodesy*, *95*(5), 51.

Xu, M. H., & Charlot, P. (2025). Variations of Absolute Source Positions Determined from Quad-band VLBI Observations. *The Astronomical Journal*, *169*(3), 173.

Xu, M. H., Heinkelmann, R., Anderson, J. M., Mora-Diaz, J., Schuh, H., & Wang, G. L. (2016). The source structure of 0642+449 detected from the CONT14 observations. *The Astronomical Journal*, *152*(5), 151.

Xu, M. H., Lunz, S., Anderson, J. M., Savolainen, T., Zubko, N., & Schuh, H. (2021b). Evidence of the *Gaia* –VLBI position differences being related to radio source structure. *Astronomy & Astrophysics*, *647*, A189.

Xu, M. H., Savolainen, T., Anderson, J. M., Kareinen, N., Zubko, N., Lunz, S., & Schuh, H. (2022). Impact of the image alignment over frequency for the VLBI Global Observing System. *Astronomy & Astrophysics*, *663*, A83.

Xu, M. H., Savolainen, T., Zubko, N., Poutanen, M., Lunz, S., Schuh, H., & Wang, G. L. (2021c). Imaging VGOS Observations and Investigating Source Structure Effects. *Journal of Geophysical Research: Solid Earth*, *126*(4), e2020JB021238.

Zubko, N., Xu, M. H., Kareinen, N., Savolainen, T., & Poutanen, M. (2025). Instrumental and systematic effects in VGOS differential ionospheric total electron content. *Advances in Space Research*, *76*(7), 3914–3930.